

# Renormalization group equations in a model of generalized hidden local symmetry and restoration of chiral symmetry

Yoshimasa Hidaka<sup>a\*</sup>, Osamu Morimatsu<sup>a†</sup> and Munehisa Ohtani<sup>b‡</sup>

<sup>a</sup>*Institute of Particle and Nuclear Studies, High Energy Accelerator Research Organization, 1-1, Oho, Tsukuba, Ibaraki, 305-0801, Japan*

<sup>b</sup>*Radiation Laboratory, RIKEN, Wako, Saitama, 351-0198, Japan*

(Dated: December 30, 2005)

We study possible restoration patterns of chiral symmetry in a generalized hidden local symmetry model, which is a low energy effective theory of QCD including pseudo-scalar, vector and axial-vector mesons. We derive Wilsonian renormalization group equations and analyze the running couplings and their fixed points at the chiral restoration point. We find three types of the chiral restoration, which are classified as the standard, vector manifestation and intermediate scenarios, respectively. It turns out that the  $\rho$  and  $A_1$  meson become massless and their decay into pion is suppressed in all the restoration patterns. The each restoration scenario violates or fulfills the vector meson dominance at the critical point in a different manner, which may reflect on the contributions from the pion to the dilepton spectrum.

PACS numbers: 11.10.Hi, 11.30.Rd, 12.39.Fe, 14.40.-n

Keywords:  $\rho$  meson, vector manifestation, hidden local symmetry, renormalization group, chiral symmetry

## I. INTRODUCTION

Dynamical chiral symmetry breaking is the most remarkable nonperturbative phenomenon in QCD together with confinement. One of the most important goals in hot and/or dense QCD is to understand how chiral symmetry restores at high temperature and/or density, which is commonly believed to be true. Then, it is crucially important to understand how hadrons change their properties in hot and/or dense matter, since it is what one observes in the actual experiments. Along these lines there have already been many theoretical as well as experimental works [1, 2, 3, 4, 5, 6, 7].

Theoretically, the properties of pseudo-scalar mesons are determined by the chiral symmetry through low-energy theorems since pseudo-scalar mesons are considered to be approximate Goldstone bosons, while the properties of other mesons are not directly controlled by the symmetry alone. An interesting possibility, the vector manifestation (VM), has recently been proposed by Harada and Yamawaki [8], in which the vector meson becomes the chiral partner of the pseudo-scalar meson when the chiral symmetry is restored and provides a theoretical basis for Brown-Rho scaling [9], i.e. the dropping of the vector-meson mass in hot and/or dense matter. The VM is based on the hidden local symmetry (HLS) by Bando et al. [10, 11, 12, 13, 14], which is a symmetry not manifest in the QCD lagrangian but is assumed to be dynamically generated, and vector mesons are introduced as gauge bosons associated with the HLS. Though there had been a long history before the work of Bando et al. [15, 16, 17, 18, 19, 20], in trying to incorporate vector mesons as gauge bosons in the low-energy effective field theory, the HLS made it possible to include vector mesons in a systematic loop expansion of the chiral perturbation theory [22].

In the broken phase of the chiral symmetry the pseudo-scalar and axial-vector mesons are mixed with each other while scalar and vector mesons are pure, when mesons are classified according to the representation associated with light-front chiral charges [27, 28, 29, 30]. This mixing is expected to vanish in the symmetric phase and the mesons form chiral doublets. It is usually believed that the scalar meson becomes the chiral partner of the pseudo-scalar meson. This is called the ‘standard scenario’. There is, however, another possibility that the longitudinal part of the vector meson becomes the chiral partner of the pseudo-scalar meson. This is the ‘VM scenario’ mentioned above. Therefore, it is an interesting question, if the VM scenario is realized in the real world or not. The VM is claimed to be realized in the HLS model at large number of flavors in ref.[8, 23, 24] by Harada and Yamawaki, at high temperature in ref.[25] by Harada and Sasaki and at high density by Harada, Kim and Rho in ref.[26]. Their argument goes as follows. The parameters of the HLS are determined from QCD by the Wilsonian matching proposed in ref.[24], namely by matching the vector and axial-vector current correlators in the HLS model with those in the operator product expansion (OPE) of QCD at the matching scale,  $\Lambda$ . Then, they obtain the parameters of the HLS at lower

---

\*Electronic address: [hidaka@post.kek.jp](mailto:hidaka@post.kek.jp)

†Electronic address: [osamu.morimatsu@kek.jp](mailto:osamu.morimatsu@kek.jp)

‡Electronic address: [ohtani@rarfaxp.riken.jp](mailto:ohtani@rarfaxp.riken.jp)

physical energy by letting the parameters run from the scale,  $\Lambda$ , according to the renormalization group equation (RGE). Now, when the chiral symmetry is restored, the vector and axial-vector current correlators must coincide with each other. When the parameters of the HLS run according to the renormalization group equation, this condition is always satisfied while the pion decay constant, which is non-zero at the matching scale,  $\Lambda$ , goes to zero at lower energy, i.e. on-shell. In the HLS model, the condition that the vector and axial-vector current correlators coincide together with the vanishing pion decay constant leads to the VM, because only the pseudo-scalar and vector mesons are included in the model [8]. Thus, it was concluded that the VM is realized in the symmetric phase.

These works, however, are not fully satisfactory in a sense that the model of the HLS includes only the pseudo-scalar and vector mesons but neither scalar nor axial-vector mesons. Namely, from the very beginning the possibility of realizing the standard scenario seems to be excluded. Thus, a natural question is what happens if one includes the axial-vector and scalar mesons into consideration. The purpose of this paper is to give a partial answer to the question by employing the generalized hidden local symmetry (GHLS) model [11, 31], which includes the axial-vector meson in addition to the pseudo-scalar and vector mesons. We analyze the renormalization group equation in the GHLS model and investigate which scenario is realized in the chiral symmetric phase. It should be noted that importance of the axial-vector meson is stressed from the viewpoint of the large  $\pi - A_1$  mixing and also of recent results of STAR collaboration [32, 33].

The paper is organized as follows. The concept of GHLS is introduced in sec. II. The Wilsonian matching for the GHLS model is performed in sec. III. The renormalization group equations and their fixed points are given in sec. IV. Possible restoration patterns are examined in sec. V. Sec. VI is devoted to the summary of the paper. The actual calculation to obtain the coefficients of the renormalization group equations is extremely complicated and only the results are shown in sec. IV. We provide the minimum necessary information in order to reproduce the results in Appendix, still which is very long.

## II. HIDDEN LOCAL SYMMETRY

The concept of the hidden local symmetry is that a symmetry, which is not manifest in the fundamental theory, is dynamically generated in the effective theory. The QCD with  $N_f$  massless quarks and its low-energy effective theory, the non-linear sigma model shares the same global symmetry,  $G_{\text{global}} = \text{SU}(N_f)_L \times \text{SU}(N_f)_R$ , under which the pion field  $U$  is transformed as

$$U \rightarrow U' = g_L U g_R^\dagger,$$

where  $g_{L,R} \in G_{\text{global}}$ . In a model of the generalized hidden local symmetry with  $G_{\text{local}} = \text{SU}(N_f)_L \times \text{SU}(N_f)_R$ , the vector and axial-vector mesons are introduced as gauge bosons associated with the hidden local symmetry [11, 31].  $G_{\text{global}} \times G_{\text{local}}$  are spontaneously broken down to global symmetry  $H_{\text{global}} = \text{SU}(N)_V$ . The vector and axial-vector mesons acquire masses through the Higgs mechanism with spontaneous breaking of the GHLS. We define representatives  $\xi_{L,R,M}$  in the quotient space  $G_{\text{global}} \times G_{\text{local}} / H_{\text{global}}$  such that  $U = \xi_L^\dagger \xi_M \xi_R$ , and hidden local gauge bosons,  $V_{L,R}$ . These fields,  $\xi_{L,R,M}$  and  $V_{L,R}$ , are transformed under  $G_{\text{global}} \times G_{\text{local}}$  as

$$\begin{aligned} \xi_{L,R} &\rightarrow \xi'_{L,R} = G_{L,R}(x) \xi_{L,R}(x) g_{L,R}^\dagger, \\ \xi_M &\rightarrow \xi'_M = G_L(x) \xi_M(x) G_R^\dagger(x), \\ V_{L,R\mu} &\rightarrow V'_{L,R\mu} = G_{L,R}(x) V_{L,R\mu} G_{L,R}^\dagger(x) - i \partial_\mu G_{L,R}(x) G_{L,R}^\dagger(x), \end{aligned} \quad (2.1)$$

$G_{L,R}(x) \in G_{\text{local}}$ . The covariant derivative for  $\xi_{L,R,M}$  are defined as

$$\begin{aligned} D_\mu \xi_L &= \partial_\mu \xi_L - i V_{L\mu} \xi_L + i \xi_L \mathcal{L}_\mu, \\ D_\mu \xi_R &= \partial_\mu \xi_R - i V_{R\mu} \xi_R + i \xi_R \mathcal{R}_\mu, \\ D_\mu \xi_M &= \partial_\mu \xi_M - i V_{L\mu} \xi_M + i \xi_M V_{R\mu}, \end{aligned} \quad (2.2)$$

where  $\mathcal{L}_\mu$  and  $\mathcal{R}_\mu$  are external gauge fields which are associated with the global symmetry  $G_{\text{global}}$ . The covariantized 1-forms,

$$\hat{\alpha}_{L,R\mu} = \frac{1}{i} D_\mu \xi_{L,R} \xi_{L,R}^\dagger, \quad \hat{\alpha}_{M\mu} = \frac{1}{2i} D_\mu \xi_M \xi_M^\dagger, \quad (2.3)$$

and field strength,

$$F_{\mu\nu}^{(L,R)} = \partial_\mu V_{L,R\nu} - \partial_\nu V_{L,R\mu} - i [V_{L,R\mu}, V_{L,R\nu}], \quad (2.4)$$

are mapped under the gauge transformations as

$$\begin{aligned}\hat{\alpha}_{L,R\mu} &\rightarrow G_{L,R}(x)\hat{\alpha}_{L,R\mu}G_{L,R}^\dagger(x), \\ \hat{\alpha}_{M\mu} &\rightarrow G_L(x)\hat{\alpha}_{M\mu}G_L^\dagger(x), \\ F_{\mu\nu}^{(L,R)} &\rightarrow G_{L,R}(x)F_{\mu\nu}^{(L,R)}G_{L,R}^\dagger(x).\end{aligned}\tag{2.5}$$

From these field and their transformations, the Lagrangian is constructed as seen in the following.

As far as the lowest-order derivative terms are concerned, the gauge invariance and even-parity condition cast the Lagrangian into the following form in general;

$$\mathcal{L}_{(2)} = aF_\pi^2 \text{tr} \hat{\alpha}_{V\mu}^2 + bF_\pi^2 \text{tr} \hat{\alpha}_{A\mu}^2 + cF_\pi^2 \text{tr} \hat{\alpha}_{M\mu}^2 + dF_\pi^2 \text{tr} (\hat{\alpha}_{A\mu} + \hat{\alpha}_{M\mu})^2,\tag{2.6}$$

where,

$$\hat{\alpha}_{V\mu} = \frac{1}{2} \left( \xi_M \hat{\alpha}_{R\mu} \xi_M^\dagger + \hat{\alpha}_{L\mu} \right), \quad \hat{\alpha}_{A\mu} = \frac{1}{2} \left( \xi_M \hat{\alpha}_{R\mu} \xi_M^\dagger - \hat{\alpha}_{L\mu} \right).\tag{2.7}$$

We can rewrite the Lagrangian by introducing  $\hat{\alpha}_{\pi\mu} \equiv \hat{\alpha}_{A\mu} + \hat{\alpha}_{M\mu}$ :

$$\begin{aligned}\mathcal{L}_{(2)} &= F_\pi^2 [\text{atr}[\hat{\alpha}_{V\mu}^2] + b \text{tr}[(\hat{\alpha}_{\pi\mu} - \hat{\alpha}_{M\mu})^2] + c \text{tr}[\hat{\alpha}_{M\mu}^2] + d \text{tr}[\hat{\alpha}_{\pi\mu}^2]] \\ &= F_\pi^2 [\text{atr}[\hat{\alpha}_{V\mu}^2] + (b+c) \text{tr}[(\hat{\alpha}_{M\mu} - \frac{b}{b+c} \hat{\alpha}_{\pi\mu})^2] + (d + \frac{bc}{b+c}) \text{tr}[\hat{\alpha}_{\pi\mu}^2]].\end{aligned}\tag{2.8}$$

By renormalizing the pion field and appropriately rewriting the coefficients we obtain

$$\mathcal{L}_{(2)} = F_\pi^2 (\text{tr}[\hat{\alpha}_{V\mu}^2] + \text{atr}[\hat{\alpha}_{V\mu}^2] + \beta \text{tr}[(\hat{\alpha}_{M\mu} - \gamma \hat{\alpha}_{\pi\mu})^2]).\tag{2.9}$$

The first term is nothing but the non-linear sigma model Lagrangian. The second and third terms correspond to mass terms for vector and axial-vector mesons.  $\pi - A_1$  mixing is controlled by the parameter,  $\gamma$ , which takes a value between 0 and 1. Unless the kinetic terms of the gauge bosons are incorporated, the Lagrangian is reduced to the non-linear sigma model as it should be in the low-energy limit. In fact, the equations of motion for  $V_\mu$  and  $A_\mu$  are given by

$$\begin{aligned}V_\mu &= \frac{1}{2} \left( \xi_{M\mu}^\dagger (\alpha_{V\mu} - \alpha_{M\mu} + \gamma \alpha_{A\mu}) \xi_{M\mu} + \alpha_{V\mu} + \alpha_{M\mu} - \gamma \alpha_{A\mu} \right), \\ A_\mu &= \frac{1}{2} \left( \xi_{M\mu}^\dagger (\alpha_{V\mu} - \alpha_{M\mu} + \gamma \alpha_{A\mu}) \xi_{M\mu} - \alpha_{V\mu} - \alpha_{M\mu} + \gamma \alpha_{A\mu} \right),\end{aligned}\tag{2.10}$$

where fields  $\alpha_{V,A,M}$  are defined as  $\hat{\alpha}_{V,A,M}$  with  $V_{L,R} = 0$ . Substituting Eq.(2.10) into the Lagrangian Eq.(2.9) leaves only the first term:  $\mathcal{L}_{(2)} = F_\pi^2 \text{tr}[\hat{\alpha}_{\pi\mu}^2]$ .

The kinetic term of gauge boson is given by

$$\begin{aligned}\mathcal{L}_{\text{kin}} &= -\frac{1}{2g^2} \text{tr}[(F_{\mu\nu}^{(L)})^2] - \frac{1}{2g^2} \text{tr}[(F_{\mu\nu}^{(R)})^2] \\ &= -\frac{1}{2g^2} \text{tr}[(F_{\mu\nu}^{(V)})^2] - \frac{1}{2g^2} \text{tr}[(F_{\mu\nu}^{(A)})^2],\end{aligned}\tag{2.11}$$

where

$$\begin{aligned}F_{\mu\nu}^{(V)} &= \partial_\mu V_\nu - \partial_\nu V_\mu - i[V_\mu, V_\nu] - i[A_\mu, A_\nu], \\ F_{\mu\nu}^{(A)} &= \partial_\mu A_\nu - \partial_\nu A_\mu - i[V_\mu, A_\nu] - i[A_\mu, V_\nu],\end{aligned}\tag{2.12}$$

with  $V_\mu = (V_{R\mu} + V_{L\mu})/2$  and  $A_\mu = (V_{R\mu} - V_{L\mu})/2$ .

Here we parameterize the nonlinear fields as

$$\begin{aligned}\xi_R(x) &= e^{-ip(x)} e^{i\sigma(x)} e^{i\pi(x)}, \\ \xi_L(x) &= e^{ip(x)} e^{i\sigma(x)} e^{-i\pi(x)}, \\ \xi_M(x) &= e^{ip(x)} e^{ip(x)}.\end{aligned}\tag{2.13}$$

By expanding the Lagrangian up to quadratic terms of these components, we obtain

$$\begin{aligned}\mathcal{L}_{\text{quad}} = & F_\pi^2 \text{tr}[(a(\partial_\mu \sigma)^2 + (1 + \beta\gamma^2)(\partial_\mu \pi)^2 + \beta(\partial_\mu p)^2 + aV_\mu^2 + \beta A_\mu^2 \\ & - 2\beta\gamma\partial^\mu \pi \partial_\mu p + 2\beta(\partial^\mu p - \gamma\partial^\mu \pi)A_\mu - 2a\partial^\mu \sigma V_\mu \\ & - 2\beta\gamma\partial^\mu p A_\mu - 2\beta\gamma A^\mu A_\mu + 2(1 + \beta\gamma^2)\partial^\mu \pi A_\mu + 2a\partial^\mu \sigma V_\mu - 2aV_\mu V^\mu + aV_\mu^2 + (1 + \beta\gamma^2)A_\mu^2],\end{aligned}\quad (2.14)$$

with  $V_\mu = (\mathcal{R}_\mu + \mathcal{L}_\mu)/2$  and  $A_\mu = (\mathcal{R}_\mu - \mathcal{L}_\mu)/2$ . Note that the field  $\pi$  in this Lagrangian cannot be interpreted as the physical pion because  $\pi$  is mixed with  $p$  through the term  $-2\beta\gamma\partial^\mu \pi \partial_\mu p$  and components of  $\pi$  are partially absorbed by  $A_\mu$ . To resolve the mixing and identify the physical pion, we shift and rescale the field as  $p \rightarrow (p/\sqrt{\beta} + \gamma\pi)/F_\pi$ , which leads us to

$$\begin{aligned}\mathcal{L}_{\text{quad}} = & \text{tr}[(\partial_\mu \sigma)^2 + (\partial_\mu \pi)^2 + (\partial_\mu p)^2 + M_\rho \rho_\mu^2 + M_{A_1}^2 A_{1\mu}^2 + 2F_p \partial^\mu p A_\mu - 2F_\sigma \partial^\mu \sigma V_\mu \\ & - 2F_{A_1} \partial^\mu p A_\mu - 2g\beta\gamma F_\pi^2 A_{1\mu}^\mu A_\mu + 2F_\pi \partial^\mu \pi A_\mu + 2F_\sigma \partial^\mu \sigma V_\mu - 2agF_\pi^2 V^\mu V_\mu + F_\sigma^2 V_\mu^2 + (F_\pi^2 + F_{A_1}^2)A_\mu^2].\end{aligned}\quad (2.15)$$

Here, other fields are also rescaled as

$$\pi \rightarrow \frac{\pi}{F_\pi}, \quad \sigma \rightarrow \frac{\sigma}{\sqrt{a}F_\pi}.\quad (2.16)$$

The gauge fields, decay constants, gauge couplings and mass of the gauge fields are expressed as

$$\begin{aligned}\rho_\mu &= gV_\mu, & A_{1\mu} &= gA_\mu, \\ F_\sigma^2 &= aF_\pi^2, & F_p^2 &= \beta F_\pi^2, & F_{A_1}^2 &= \beta\gamma^2 F_\pi^2, \\ M_\rho^2 &= ag^2 F_\pi^2, & M_{A_1}^2 &= \beta g^2 F_\pi^2.\end{aligned}\quad (2.17)$$

### III. WILSONIAN MATCHING FOR THE GHLS

Since the GHLS model is an effective theory of QCD, the parameters of the GHLS model can and should be determined from QCD. In this section we apply the Wilsonian matching for the GHLS model [24, 35]. Following ref.[24, 35], we adjust the vector and axial-vector current correlators in the GHLS model to the correlators in QCD calculated by the operator product expansion (OPE). Here we assume the existence of an energy scale,  $\Lambda$ , above  $A_1$  meson mass where both the GHLS model and the OPE of QCD are applicable.

The vector and axial-vector current correlators are defined by

$$\begin{aligned}i \int d^4x e^{ipx} \langle 0 | T J_\mu^a(x) J_\nu^b(0) | 0 \rangle &= -\delta^{ab} P^{\mu\nu} \Pi_V(Q^2), \\ i \int d^4x e^{ipx} \langle 0 | T J_{5\mu}^a(x) J_{5\nu}^b(0) | 0 \rangle &= -\delta^{ab} P^{\mu\nu} \Pi_A(Q^2),\end{aligned}\quad (3.1)$$

where  $Q^2 = -p^2$  and  $P^{\mu\nu} = g^{\mu\nu}p^2 - p^\mu p^\nu$ . These correlators are well described by the tree-level contributions around the matching scale,  $\Lambda$  [24, 35]. In the GHLS model, the correlators up to  $\mathcal{O}(p^4)$  are given by

$$\begin{aligned}\Pi_A^{(\text{GHLS})}(Q^2) &= \frac{F_\pi^2(\Lambda)}{Q^2} + \frac{F_{A_1}^2(\Lambda)(1 - g_{A_1}^2(\Lambda)z_4(\Lambda)/\gamma(\Lambda))}{M_{A_1}^2(\Lambda) + Q^2} - 2z_2(\Lambda), \\ \Pi_V^{(\text{GHLS})}(Q^2) &= \frac{F_\sigma^2(\Lambda)(1 - 2g_\rho^2(\Lambda)z_3(\Lambda))}{M_\rho^2(\Lambda) + Q^2} - 2z_1(\Lambda),\end{aligned}\quad (3.2)$$

where  $g_\rho^2(\Lambda) = g^2(\Lambda)/(1 + 2\kappa(\Lambda))$ ,  $g_{A_1}^2(\Lambda) = g^2(\Lambda)/(1 - 2\kappa(\Lambda))$ ,  $M_\rho^2(\Lambda) = g_\rho^2(\Lambda)F_\sigma^2(\Lambda)$  and  $M_{A_1}^2(\Lambda) = g_{A_1}^2(\Lambda)F_p^2(\Lambda)$ .  $\kappa$ ,  $z_1$ ,  $z_2$ ,  $z_3$  and  $z_4$  are coefficients in the following Lagrangian of  $\mathcal{O}(p^4)$ :

$$\begin{aligned}\mathcal{L}_{(4)z} = & \frac{\kappa}{2g^2} \text{tr}[F_{\mu\nu}^{(L)} \xi_M F^{(R)\mu\nu} \xi_M^\dagger] + \frac{z_1 + z_2}{4} \text{tr}[(\mathcal{F}_{\mu\nu}^{(L)})^2 + (\mathcal{F}_{\mu\nu}^{(R)})^2] + \frac{z_1 - z_2}{2} \text{tr}[\mathcal{F}_{\mu\nu}^{(L)} \xi_L^\dagger \xi_M \xi_R \mathcal{F}^{(R)\mu\nu} \xi_R^\dagger \xi_M^\dagger \xi_L] \\ & + \frac{z_3 + z_4}{4} \text{tr}[\xi_L \mathcal{F}_{\mu\nu}^{(L)} \xi_L^\dagger F^{(L)\mu\nu} + \xi_R \mathcal{F}_{\mu\nu}^{(R)} \xi_R^\dagger F^{(R)\mu\nu}] + \frac{z_3 - z_4}{4} \text{tr}[\mathcal{F}_{\mu\nu}^{(L)} \xi_L^\dagger \xi_M F^{(R)\mu\nu} \xi_M^\dagger \xi_L + \mathcal{F}_{\mu\nu}^{(R)} \xi_R^\dagger \xi_M F^{(L)\mu\nu} \xi_M^\dagger \xi_R].\end{aligned}\quad (3.3)$$

On the other hand, the OPE in QCD leads to the correlators up to  $\mathcal{O}(1/Q^6)$  [36, 37] as

$$\begin{aligned}\Pi_{\mathcal{A}}^{(\text{QCD})}(Q^2) &= \frac{1}{8\pi^2} \left( - \left( 1 + \frac{\alpha_s}{\pi} \right) \ln \frac{Q^2}{\mu^2} + \frac{\pi\alpha_s}{3} \frac{\langle G_{\mu\nu} G^{\mu\nu} \rangle}{Q^4} + \frac{1408\pi^3\alpha_s}{81} \frac{\langle \bar{q}q \rangle^2}{Q^6} \right), \\ \Pi_{\mathcal{V}}^{(\text{QCD})}(Q^2) &= \frac{1}{8\pi^2} \left( - \left( 1 + \frac{\alpha_s}{\pi} \right) \ln \frac{Q^2}{\mu^2} + \frac{\pi\alpha_s}{3} \frac{\langle G_{\mu\nu} G^{\mu\nu} \rangle}{Q^4} - \frac{896\pi^3\alpha_s}{81} \frac{\langle \bar{q}q \rangle^2}{Q^6} \right),\end{aligned}\quad (3.4)$$

where  $\mu$  is the renormalization scale of QCD.

Now let us make the Wilsonian matching of Eq.(3.2) with Eq.(3.4) at the scale  $\Lambda$ . We note that the correlators in Eq.(3.4) explicitly depend on the renormalization scale  $\mu$ . To eliminate the explicit  $\mu$  dependence, we consider the difference,  $\Pi_{\mathcal{A}} - \Pi_{\mathcal{V}}$ , and the first derivative of the correlators. Then the matching condition for the difference is

$$\left( \Pi_{\mathcal{A}}^{(\text{GHLS})}(Q^2) - \Pi_{\mathcal{V}}^{(\text{GHLS})}(Q^2) \right) \Big|_{Q^2=\Lambda^2} = \left( \Pi_{\mathcal{A}}^{(\text{QCD})}(Q^2) - \Pi_{\mathcal{V}}^{(\text{QCD})}(Q^2) \right) \Big|_{Q^2=\Lambda^2} = \frac{32\pi\alpha_s}{9} \frac{\langle \bar{q}q \rangle^2}{\Lambda^6}. \quad (3.5)$$

The matching conditions of the first derivative for each  $\Pi_{\mathcal{A},\mathcal{V}}$  are given by

$$-Q^2 \frac{d}{dQ^2} \Pi_{\mathcal{A},\mathcal{V}}^{(\text{GHLS})}(Q^2) \Big|_{Q^2=\Lambda^2} = -Q^2 \frac{d}{dQ^2} \Pi_{\mathcal{A},\mathcal{V}}^{(\text{QCD})}(Q^2) \Big|_{Q^2=\Lambda^2}, \quad (3.6)$$

where

$$\begin{aligned}-Q^2 \frac{d}{dQ^2} \Pi_{\mathcal{A}}^{(\text{GHLS})}(Q^2) \Big|_{Q^2=\Lambda^2} &= \frac{F_\pi^2(\Lambda)}{\Lambda^2} + \frac{\Lambda^2 F_{A_1}^2(\Lambda)(1 - 2g_{A_1}^2(\Lambda)z_4(\Lambda)/\gamma(\Lambda))}{(\Lambda^2 + M_{A_1}^2(\Lambda))^2}, \\ -Q^2 \frac{d}{dQ^2} \Pi_{\mathcal{V}}^{(\text{GHLS})}(Q^2) \Big|_{Q^2=\Lambda^2} &= \frac{\Lambda^2 F_\sigma^2(\Lambda)(1 - 2g_\rho^2(\Lambda)z_3(\Lambda))}{(\Lambda^2 + M_\rho^2(\Lambda))^2},\end{aligned}\quad (3.7)$$

and

$$\begin{aligned}-Q^2 \frac{d}{dQ^2} \Pi_{\mathcal{A}}^{(\text{QCD})}(Q^2) \Big|_{Q^2=\Lambda^2} &= \frac{1}{8\pi^2} \left( 1 + \frac{\alpha_s}{\pi} + \frac{2\pi\alpha_s}{3} \frac{\langle G_{\mu\nu} G^{\mu\nu} \rangle}{\Lambda^4} + \frac{1408\pi^3\alpha_s}{27} \frac{\langle \bar{q}q \rangle^2}{\Lambda^6} \right), \\ -Q^2 \frac{d}{dQ^2} \Pi_{\mathcal{V}}^{(\text{QCD})}(Q^2) \Big|_{Q^2=\Lambda^2} &= \frac{1}{8\pi^2} \left( 1 + \frac{\alpha_s}{\pi} + \frac{2\pi\alpha_s}{3} \frac{\langle G_{\mu\nu} G^{\mu\nu} \rangle}{\Lambda^4} - \frac{896\pi^3\alpha_s}{27} \frac{\langle \bar{q}q \rangle^2}{\Lambda^6} \right).\end{aligned}\quad (3.8)$$

When the chiral symmetry is restored, the vector current correlator coincides with the axial one due to  $\langle \bar{q}q \rangle \rightarrow 0$ :

$$\left( \Pi_{\mathcal{A}}^{(\text{GHLS})}(Q^2) - \Pi_{\mathcal{V}}^{(\text{GHLS})}(Q^2) \right) \Big|_{Q^2=\Lambda^2} \rightarrow 0. \quad (3.9)$$

The derivatives of the vector and axial-vector correlators of Eq.(3.8) become also identical with each other. We emphasize that their values are finite but nonzero because  $(\alpha_s/\pi)\langle G_{\mu\nu} G^{\mu\nu} \rangle$  may not vanish at the restoration point. This implies

$$\begin{aligned}F_\pi^2(\Lambda) + \frac{F_{A_1}^2(\Lambda)(1 - 2g_{A_1}^2(\Lambda)z_4(\Lambda)/\gamma(\Lambda))}{(1 + M_{A_1}^2(\Lambda)/\Lambda^2)^2} &\neq 0, \\ F_\sigma^2(\Lambda)(1 - 2g_\rho^2(\Lambda)z_3(\Lambda)) &\neq 0.\end{aligned}\quad (3.10)$$

With the parameters obtained by the Wilsonian matching, the low-energy parameters such as on-shell  $\rho$  meson mass are derived by the renormalization group. We discuss more detail of the restoration of chiral symmetry in sec.V.

#### IV. RENORMALIZATION GROUP EQUATIONS

In the HLS model, quantum effects on couplings have been studied by the renormalization group [23, 34]. It was pointed out that the quadratic divergence plays an important role in the chiral transition, especially in connection with the large  $N_f$  QCD [23]. Quantum corrections to the bare parameters suggest a violation of the vector meson dominance. Following this argument in the HLS model, we consider the renormalization group for the couplings in the

GHLS model to estimate quantum effects and find fixed points. To this end, we introduce dimensionless parameters for convenience;

$$x(\mu) = \frac{N_f}{(4\pi)^2} \frac{\mu^2}{F_\pi^2(\mu)}, \quad G(\mu) = \frac{N_f}{(4\pi)^2} g^2(\mu). \quad (4.1)$$

By calculating one-loop diagrams contributing to the bare couplings as shown in Appendix, we obtain renormalization group equations for the parameters as

$$\begin{aligned} \mu \frac{dx}{d\mu} &= x \left\{ 2 - x \left( 2 - a + 2\gamma^2 + 2a\gamma^2 - \frac{a\gamma^2}{\beta} - \frac{\beta\gamma^2}{a} - a\gamma^4 \right) \right. \\ &\quad \left. + \frac{3}{2}G \left( a^2 - a\gamma^2 - 2a^2\gamma^2 + \frac{a^2\gamma^2}{\beta} - \beta\gamma^2 + \frac{\beta^2\gamma^2}{a} + a^2\gamma^4 \right) \right\}, \\ \mu \frac{da}{d\mu} &= x \left( \frac{1}{2} - 2a + \frac{3a^2}{2} + \frac{a^2}{2\beta^2} - 2a\gamma^2 - 3a^2\gamma^2 + \frac{2a^2\gamma^2}{\beta} + \frac{3a^2\gamma^4}{2} \right) \\ &\quad + \frac{3}{2}Ga \left( 1 - a^2 + \frac{a}{\beta} + 2a\gamma^2 + 2a^2\gamma^2 - \frac{a^2\gamma^2}{\beta} - \beta\gamma^2 - a^2\gamma^4 \right), \\ \mu \frac{d\beta}{d\mu} &= x \left( 2 - \frac{a}{\beta} - 2\beta + a\beta - 2\beta\gamma^2 - 2a\beta\gamma^2 + \frac{2\beta^2\gamma^2}{a} + a\beta\gamma^4 \right) \\ &\quad + \frac{3}{2}G \left( -3a + \frac{a^2}{\beta} + 4\beta - a^2\beta - a\beta\gamma^2 + 2a^2\beta\gamma^2 + 2\beta^2\gamma^2 - \frac{\beta^3\gamma^2}{a} - a^2\beta\gamma^4 \right), \\ \mu \frac{d\gamma^2}{d\mu} &= 2x\gamma^2 \left( \frac{1}{a} + \frac{a}{\beta^2} - \frac{2}{\beta} - \frac{a}{\beta} + \frac{a\gamma^2}{\beta} \right) + 3G\gamma^2 \left( -1 - a - \frac{a^2}{\beta^2} + \frac{2a}{\beta} + \frac{a^2}{\beta} + a\gamma^2 - \frac{a^2\gamma^2}{\beta} \right), \\ \mu \frac{dG}{d\mu} &= -G^2 \left\{ \frac{44}{3} - \frac{1}{24} \left( 5 + a^2 + \frac{a^2}{\beta^2} - \frac{2a}{\beta} - 2a\gamma^2 - 2a^2\gamma^2 + \frac{2a^2\gamma^2}{\beta} - 2\beta\gamma^2 + \frac{2\beta^2\gamma^2}{a} + a^2\gamma^4 \right) \right\}. \end{aligned} \quad (4.2)$$

If we take a limit of  $\beta \rightarrow \infty$  and  $\gamma \rightarrow 0$ , the above RGEs for  $x$  and  $a$  do not receive contributions from the  $A_1$  meson and are reduced to those in the HLS model. However, it is not the case for  $G$ , because the number of the gauge fields in the GHLS model is different from that in the HLS model and the loop contributions of the field  $p$  remain in the limit. This is due to the cancellation between the overall decay constants in the Lagrangian and denominators in the power series of the fields. In the next section we examine these equations for fixed points to discuss the properties on the chiral-transition point.

## V. RESTORATION PATTERN

The chiral restoration is characterized by the condition that the on-shell pion decay constant vanishes,  $F_\pi(0) \rightarrow 0$ . That is to say the non-vanishing of the dimensionless parameter  $x(\mu)$  defined in Eq.(4.1) in the low-energy limit:

$$x(0) \neq 0. \quad (5.1)$$

Inversely,  $x(0) = 0$  means a broken phase because of  $F_\pi(0) \neq 0$  and is excluded from the parameter sets associated with the restoration point. In addition to Eq.(5.1), we analyze the restoration patterns of chiral symmetry using the vector and axial-vector current correlators. When the chiral symmetry is restored, the vector current correlator should be equal to the axial vector one, not only at the matching scale  $\Lambda$  as shown in Eq.(3.9) but also at the low-energy region less than  $\Lambda$ . Accordingly, at the restoration point we require equality of these correlators;

$$\Pi_V(Q^2) = \Pi_A(Q^2), \quad (5.2)$$

for  $Q^2 \leq \Lambda^2$ . Since the HLS model includes of only  $\pi$  and  $\rho$ , the equality of correlators and Wilsonian matching uniquely bring about the VM scenario [8, 35]. In the GHLS model, however, other possibilities exist. Actually considering the restraints on the decay constants of Eq.(3.10), Eq.(5.2) gives  $z_1(\mu) = z_2(\mu)$  and preserves the following three possibilities:

$$(I) \quad M_\rho^2(\mu) = M_{A_1}^2(\mu), \quad F_{A_1}^2(\mu)(1 - 2g_{A_1}^2(\mu)z_4(\mu)) = F_\sigma^2(\mu)(1 - 2g_\rho^2(\mu)z_3(\mu)) \quad \text{and} \quad F_\pi^2(\mu) = 0, \quad (5.3)$$

$$(II) \quad M_\rho^2(\mu) = 0, \quad F_\sigma^2(\mu)(1 - 2g_\rho^2(\mu)z_3(\mu)) = F_\pi^2(\mu) \quad \text{and} \quad F_{A_1}^2(\mu)(1 - 2g_{A_1}^2(\mu)z_4(\mu)/\gamma(\mu)) = 0, \quad (5.4)$$

$$(III) \quad M_\rho(\mu) = M_{A_1}(\mu) = 0 \quad \text{and} \quad F_\pi^2(\mu) = F_\sigma^2(\mu)(1 - 2g_\rho^2(\mu)z_3(\mu)) - F_{A_1}^2(\mu)(1 - 2g_{A_1}^2(\mu)z_4(\mu)/\gamma(\mu)). \quad (5.5)$$

In order to determine whether each of the above possibilities can be realized, we require that the restoration condition is satisfied for any energy below the matching scale. This demands that each of Eqs. (5.3)-(5.5) is renormalization-group invariant.

Let us begin with the case (I). Eq. (5.3),  $F_\pi^2(\mu) = 0$  implies that the power expansion of  $p^2/(4\pi F_\pi(\Lambda))^2$  breaks down. Therefore, the first possibility is inconsistent with the one-loop approximation adopted in this analysis and is not studied further.

Next, we consider the case (II). From Eq. (5.4) we obtain

$$g^2 = 0, \quad a = 1, \quad \beta\gamma^2 = 0, \quad (5.6)$$

for any  $\mu$  less than the matching scale. Since the renormalization group equations for these quantities are rendered as

$$\mu \frac{dG}{d\mu} = 0, \quad \mu \frac{da}{d\mu} = x \frac{1}{2\beta^2}, \quad \mu \frac{d(\beta\gamma^2)}{d\mu} = x\gamma^2(-4 + \frac{1}{\beta} + 2\gamma^2), \quad \mu \frac{d(z_1 - z_2)}{d\mu} = \frac{N_f}{(4\pi)^2} \frac{1}{24\beta^2}, \quad (5.7)$$

Eq.(5.6) with  $z_1(\mu) = z_2(\mu)$  results in  $\beta \rightarrow \infty$  and  $\gamma = 0$  for any  $\mu$ . As we take a low energy limit  $\mu \rightarrow 0$ , other parameters are also expected to be in a fixed point. Considering the above conditions together with the RGE for  $x$

$$\mu \frac{dx}{d\mu} = x(2 - x), \quad (5.8)$$

the non-trivial fixed point is found to be  $(x, a, \beta, \gamma^2, G) = (2, 1, \infty, 0, 0)$ . This fixed point corresponds to the VM, in which  $M_\rho \rightarrow M_\pi = 0$  and  $F_\sigma/F_\pi \rightarrow 1$ . We note that a combination of  $\beta\gamma^2$  remains to be zero as  $\beta \rightarrow \infty$  and  $\gamma \rightarrow 0$  from Eq.(5.6) and hence  $F_{A_1} = 0$ . We can say that  $A_1$  is decoupled to the system in this case and the GHLS model is reduced to the HLS model at the restoration point.

Finally, we discuss the case (III). Note that the second condition of Eq.(5.5) is nothing but the first Weinberg sum rule which is saturated by the pole terms [38]. From Eq.(5.5) we obtain

$$g^2 = 0 \quad \text{and} \quad a - \beta\gamma^2 - 1 = 0, \quad (5.9)$$

for any  $\mu$  less than the matching scale. The RGEs for these quantities are given by

$$\mu \frac{dG}{d\mu} = 0, \quad \mu \frac{d(a - \beta\gamma^2 - 1)}{d\mu} = -x \frac{(1 - \gamma^2)a^2 - 2a + 1}{2(1 - a)^2}, \quad \mu \frac{d(z_1 - z_2)}{d\mu} = \frac{N_f}{(4\pi)^2} \frac{(1 - \gamma^2)a^2 - 2a + 1}{24(1 - a)^2}. \quad (5.10)$$

From these, we can see that a parameter set of  $a = 1/(1 - \gamma)$  and  $\beta = 1/((1 - \gamma)\gamma)$  makes Eq.(5.9) invariant under the renormalization group. Here we note that this parameter set satisfies the first and second Weinberg sum rules at  $\mathcal{O}(p^2)$  even if we take a nonzero  $g$  [39]. Under these conditions, remaining RGEs for  $x$  and  $\gamma^2$  become

$$\mu \frac{dx}{d\mu} = x(2 - (1 - 2\gamma + 3\gamma^2)x), \quad \mu \frac{d\gamma^2}{d\mu} = 2\gamma^2(1 - \gamma)(1 - 3\gamma)x. \quad (5.11)$$

The parameters  $x$  and  $\gamma$  are expected to be in a fixed point in the low energy limit of  $\mu \rightarrow 0$ . Except for the trivial fixed point of  $x = 0$  with an arbitrary  $\gamma$ , we find three fixed points from Eq.(5.11),

$$(x, \gamma) = \begin{cases} (1, 1) & \text{(the standard type)} \\ (2, 0) & \text{(the VM type)} \\ (3, 1/3) & \text{(the intermediate type)}. \end{cases} \quad (5.12)$$

These fixed points are classified into the restoration types noted above according to the value of  $\gamma$ , because the  $\pi$ - $A_1$  mixing are basically controlled by  $\gamma$  as discussed in the next subsection. The parameters below the matching scale and the fixed points are summarized for each restoration pattern in Table I.

Under the standard scenario, if  $a$  was in a fixed point at the matching scale,  $F_\sigma(\Lambda)$  would diverge and be inconsistent with Eq.(3.10) because  $F_\sigma(\Lambda)$  must be finite. Thus we do not claim that the parameters are fixed on a fixed point at the matching scale. Under the VM scenario in the case of (II), the parameters are on a fixed point and  $\gamma$  keeps taking zero for  $\mu$  lower than the matching scale. However, for the VM in the case of (III),  $\gamma$  does not vanish for a non-zero  $\mu$  and is not on any fixed points. Consequently, in the case of (II)  $A_1$  is decoupled in the bare Lagrangian, while for the VM in case of (III)  $A_1$  remains to be dynamical at least near the matching scale. This difference is expected to reflect on the spectrum of  $A_1$  as the chiral symmetry is restored.

|                                      | $0 < \mu \leq \Lambda$  | fixed point ( $\mu \rightarrow 0$ ) |          |          |          |                    |                    |
|--------------------------------------|---|-------------------------------------|----------|----------|----------|--------------------|--------------------|
|                                      |   | $x$                                 | $a$      | $\beta$  | $\gamma$ | $\psi$             | $g_{\gamma\pi\pi}$ |
| (II) VM                              | $a = 1, \beta = \infty, \gamma = 0$ ( $\beta\gamma^2 = 0$ )                       | 2                                   | 1        | $\infty$ | 0        | 0                  | 1/2                |
| (III) VM<br>Standard<br>Intermediate | $\begin{cases} a = 1/(1 - \gamma), \\ \beta = 1/(\gamma(1 - \gamma)) \end{cases}$ | 2                                   | 1        | $\infty$ | 0        | 0                  | 1/2                |
|                                      |   | 1                                   | $\infty$ | $\infty$ | 1        | $\pi/2$            | 0                  |
|                                      |   | 3                                   | 3/2      | 9/2      | 1/3      | $\arctan \sqrt{2}$ | 1/3                |

TABLE I: Parameters and their fixed points for the restoration patterns. The gauge coupling is zero,  $g = 0$ , for these restoration patterns. In the intermediate scenario, the fixed point is not realized in the limit of  $\mu \rightarrow 0$  unless the parameters are adjusted at the matching scale.

Although the parameters may not be located on the fixed point at the matching scale, the couplings must be on the critical line along which the renormalization-group flow enters into an infrared fixed point satisfying  $x(0) \neq 0$ . The intermediate fixed point is on the critical line but an UV fixed point. It requires a fine adjustment to keep the point realized in IR region, but no reason exists to justify such an adjustment. The restoration conditions put severe constraints on the couplings, and without these conditions all of the fixed points become unstable. Unless Eq.(5.1) is satisfied, a fixed point of the vector realization defined as  $x = 0$  with Eq.(5.2) will be achieved [40].

It turns out that the gauge coupling becomes zero,  $g = 0$ , at the all fixed points satisfying the restoration condition. This fact implies that  $\rho$  and  $A_1$  get lighter as the chiral symmetry is restored and eventually become massless at the restoration point. This result is consistent with the Brown-Rho scaling [9].

### A. The mixing angle

When mesons are classified by the light-front charge of the chiral group  $SU(N_f)_L \times SU(N_f)_R$  in the broken phase, the spontaneous breaking of the chiral symmetry mixes the pseudo-scalar meson with the longitudinal part of the axial-vector meson while the scalar and vector mesons remain to be pure representations:

$$\begin{aligned}
|\sigma\rangle &= |(N_f^2 - 1, 1) \oplus (1, N_f^2 - 1)\rangle, \\
|\pi\rangle &= |(N_f, N_f^*) \oplus (N_f^*, N_f)\rangle \sin \psi + |(N_f^2 - 1, 1) \oplus (1, 8)\rangle \cos \psi, \\
|\rho\rangle &= |(N_f, N_f^*) \oplus (N_f^*, N_f)\rangle, \\
|A_1\rangle &= |(N_f, N_f^*) \oplus (N_f^*, N_f)\rangle \cos \psi - |(N_f^2 - 1, 1) \oplus (1, N_f^2 - 1)\rangle \sin \psi.
\end{aligned} \tag{5.13}$$

The experimental values of the decay constants suggest that the mixing angle,  $\psi$ , takes  $\psi \simeq \pi/4$  assuming two light flavors [27, 28]. As the chiral symmetry is restored, the mixing is expected to disappear and physical states become pure representations because the light-front chiral charge commutes with the Hamiltonian [30]. It is non-trivial to which representation the pion belongs. In the case that the pion belongs to  $(N_f, N_f^*) \oplus (N_f^*, N_f)$  with  $\psi = \pi/2$ , the scalar meson becomes the chiral partner of the pion and we call it the standard scenario of the chiral restoration. In the case that the pion belongs to  $(N_f^2 - 1, 1) \oplus (1, N_f^2 - 1)$  with  $\psi = 0$ , the pion and the longitudinal mode of the  $\rho$  meson form a doublet, which is called the VM scenario [8].

In this section, we determine the mixing angle at the restoration point for each restoration pattern classified in the above. We define the mixing angle in the GHLS model as the ratio of the pole residues for  $\pi$  and  $A_1$  in the axial-vector current correlator. These residues correspond to  $\pi$  and  $A_1$  decay constants squared and the mixing angle is expressed as

$$\tan^2 \psi = \frac{F_{A_1}^2(M_{A_1}^2)(1 - g_{A_1}^2(M_{A_1}^2)z_4(M_{A_1}^2)/\gamma(M_{A_1}^2))}{F_\pi^2(0)} = \beta(M_{A_1}^2)\gamma^2(M_{A_1}^2)(1 - g_{A_1}^2(M_{A_1}^2)z_4(M_{A_1}^2)/\gamma(M_{A_1}^2)). \tag{5.14}$$

At the restoration point, this expression becomes

$$\tan^2 \psi = \beta(0)\gamma^2(0), \tag{5.15}$$

due to  $M_{A_1} = 0$  and  $g_{A_1} = 0$ . Therefore the mixing angle is controlled by the infrared behavior of the parameters near the restoration point. Corresponding to the three fixed points discussed in the previous section, the mixing angle at the restoration point is given by

$$\text{Standard : } \tan \psi \rightarrow \infty, \quad \text{VM : } \tan \psi \rightarrow 0, \quad \text{Intermediate : } \tan \psi \rightarrow \sqrt{2}. \tag{5.16}$$



As is expected, the mixing disappears at the standard and VM fixed points, but survives at the intermediate fixed point. The intermediate fixed point should be excluded if we require that the mixing of  $\pi$  and  $A_1$  is resolved at the restoration point.

### B. Pion form factor and vector meson dominance

The vector meson dominance (VMD) for the pion form factor is well established in the vacuum [16]. The pion form factor in the GHLS model is written up to  $\mathcal{O}(p^2)$  as

$$F_V^{\pi^\pm}(p^2) = \left(1 - \frac{a}{2}(1 - \gamma^2)\right) + \frac{a}{2}(1 - \gamma^2) \frac{M_\rho^2}{M_\rho^2 - p^2}. \quad (5.17)$$

The first term is the direct term,  $g_{\gamma\pi\pi}$ , and the second term is the  $\rho$  meson exchange term. The VMD implies

$$g_{\gamma\pi\pi} = 1 - \frac{a}{2}(1 - \gamma^2) \approx 0. \quad (5.18)$$

At the chiral restoration point, this coupling is expressed as

$$g_{\gamma\pi\pi}(\mu) = \frac{1 - \gamma(\mu)}{2}$$

and its behavior at low energy is different according to the restoration patterns classified above. Under the VM scenario in the case of (II)  $g_{\gamma\pi\pi}$  takes a constant value of 1/2. In the case of (III), the coupling runs depending on the parameter  $\gamma$  and shows (in)violation of the VMD in the infrared limit as

$$g_{\gamma\pi\pi} \rightarrow \begin{cases} 0 & \text{(the standard type)} \\ 1/2 & \text{(the VM type)} \\ 1/3 & \text{(the intermediate type)} \end{cases} \quad \text{as } \mu \rightarrow 0. \quad (5.19)$$

In the standard scenario the VMD is satisfied. The violation of VMD appears in the VM and Intermediate fixed points.

On the other hand,  $g_{\rho\pi\pi}$  coupling is written by

$$g_{\rho\pi\pi} = \frac{g}{2}a(1 - \gamma^2). \quad (5.20)$$

The coupling  $g_{\rho\pi\pi}$  becomes weaker as chiral symmetry is restored for all restoration patterns because the gauge coupling diminishes. This implies that  $\rho$  becomes stable for the decay into two pions near the restoration point and makes a sharp peak in the dilepton spectrum on the background from pions, universally.

The difference among the restoration patterns may be reflected on the pion background through the violation of the VMD. The pion background in the dilepton spectrum is suppressed in the standard scenario, while the large violation of the VMD leads to an enhancement of the background in the VM scenario. Thus observations of the dilepton spectrum in the vector channel near the restoration point will ascertain the validity of the GHLS model adopted here as well as the true restoration pattern in the real world.

## VI. SUMMARY

In this paper we have studied possible patterns of chiral restoration employing the GHLS model, which includes the axial-vector meson in addition to the pseudo-scalar and vector mesons. First, we obtained constraints on the parameters of the GHLS by matching the vector and axial-vector correlators of the GHLS model with those in the operator product expansion of QCD at a matching scale,  $\Lambda$ . Next, we derived renormalization group equations for the GHLS model by calculating one-loop corrections to the two-point functions. Then, we examined behavior of the parameters at low energy and searched for fixed points of them at the restoration point by the obtained renormalization group equations. As the restoration conditions, we required the equality of the vector and axial-vector correlators and the vanishing of the on-shell pion decay constant.

We found four patterns of the running parameters at the restoration point which flow to three fixed points. The first fixed point correspond to the ‘standard scenario’, in which the vector and axial-vector mesons are degenerate.

The second one is the ‘vector manifestation scenario’, in which the longitudinal part of the vector meson and the pseudo-scalar meson are degenerate. In both these scenarios, the mixing of two representations associated with  $\pi$  and  $A_1$  mesons diminishes at the restoration point as expected. On the other hand, the third fixed-point is of a new type, which can be regarded as the ‘intermediate scenario’ in a sense that the mixing remains even at the restoration point. It is noted, however, that this fixed point is not an infrared one and will not be achieved unless the parameters are perfectly adjusted to the point at the matching scale.

In each of the restoration patterns, both  $\rho$  and  $A_1$  are expected to become massless, since the gauge coupling vanishes at the restoration point. It is further expected that the vector meson becomes stable because the coupling constant,  $g_{\rho\pi\pi}$ , also vanishes and the decay into pions is suppressed at the restoration point. Here we emphasize that these results are universal to all restoration patterns. These three scenarios, however, are different in the violation of the vector meson dominance. This difference will be reflected on the pion background in the spectrum of dilepton decay from the vector meson. Two restoration patterns running into the VM fixed point are also distinguished through the  $A_1$  spectrum near the restoration point owing to the different behavior of parameters at low energy.

Now, a crucial question is whether these fixed points are physically realized or not. It is determined if one can reach the restoration points continuously as one approaches the critical temperature or density of chiral restoration. The application to the system of finite temperature and/or density is our future problem.

We would like to mention here possible phenomenological consequences of the results of the present work. The dropping of the  $\rho$  meson mass implies the threshold enhancement in the  $\rho$  meson spectrum at some temperature and/or density because the  $\rho$  meson mass is expected to coincide with twice the pion mass, which is analogous to the enhancement of the sigma spectrum [41] in the standard scenario studied within the linear sigma model [42, 43]. (Here, explicit breaking of chiral symmetry is taken into consideration and the pion is supposed to have a small finite mass.)

Another point to be mentioned is that the GHLS model does not include the scalar meson, which becomes the chiral partner of the pseudo-scalar meson in the standard scenario. To include the scalar meson in the analysis is therefore another important future problem.

## Acknowledgment

We would like to thank Prof. M. Harada for useful discussions.

## Note added

After finishing up this work we became aware of similarly work by Harada and Sasaki [39]. Although their analysis takes a different parameterization and gauge fixing from ours, obtained renormalization group equations and results are consistent with our work.

## APPENDIX A: GAUGE FIXING

We take a gauge fixing to calculate quantum corrections. We perform a  $R_\xi$  like BRS quantization. The BRS transformations are defined by

$$\begin{aligned}
\delta_B \xi_{V,A} &= iC_V \xi_{V,A} + iC_A \xi_{A,V}, \\
\delta_B \xi_M &= i(C_V - C_A) \xi_M - i\xi_M (C_V + C_A), \\
\delta_B V_\mu &= \partial_\mu C_V + i[C_V, V_\mu] + i[C_A, A_\mu] = D_\mu C_V, \\
\delta_B A_\mu &= \partial_\mu C_A + i[C_V, A_\mu] + i[C_A, V_\mu] = D_\mu C_A, \\
\delta_B C_{V,A} &= i(C_V C_{V,A} + C_A C_{A,V}), \\
\delta_B \bar{C}_{V,A} &= iB_{V,A}, \\
\delta_B B_{V,A} &= 0,
\end{aligned} \tag{A.1}$$

where  $C_{V,A}$  and  $\bar{C}_{V,A}$  are the Faddeev Popov ghost field,  $B_{V,A}$  is the Nakanishi-Lautrup (NL) field, and

$$\xi_{V,A} = \frac{1}{2}(\xi_R \pm \xi_L). \tag{A.2}$$

We choose the gauge fixing function as follows

$$F = \text{tr}[\bar{C}_V(\partial^\mu V_\mu + \alpha_V G_V + \frac{1}{2}\alpha_V B_V)] + \text{tr}[\bar{C}_A(\partial^\mu A_\mu + \alpha_A G_A + \frac{1}{2}\alpha_A B_A)], \tag{A.3}$$

where

$$\begin{aligned}
G_V &= \frac{aF_\pi^2}{2i}(\xi_V - \xi_V^\dagger), \\
G_A &= \frac{\beta F_\pi^2}{2i}(\gamma(\xi_A - \xi_A^\dagger + \xi_{M-}) - \xi_{M-}), \\
\xi_{M\pm} &= \frac{1}{2}(\xi_M \pm \xi_M^\dagger).
\end{aligned} \tag{A.4}$$

We obtain the gauge-fixing and FP terms:

$$\begin{aligned}
\mathcal{L}_{\text{GF}} + \mathcal{L}_{\text{FP}} &= -i\delta_B F, \\
\mathcal{L}_{\text{GF}} &= 2\text{tr}[B_V(\partial^\mu V_\mu + \alpha_V G_V + \frac{1}{2}\alpha_V B_V)] + 2\text{tr}[B_A(\partial^\mu A_\mu + \alpha_A G_A + \frac{1}{2}\alpha_A B_A)], \\
\mathcal{L}_{\text{FP}} &= 2i\text{tr}[\bar{C}_V(\partial^\mu D_\mu C_V + \alpha_V G'_V)] + 2i\text{tr}[\bar{C}_A(\partial^\mu D_\mu C_A + \alpha_A G'_A)], \\
G'_V &= \delta_B G_V = \frac{aF_\pi^2}{2}(C_V \xi_V + \xi_V^\dagger C_V + C_A \xi_A + \xi_A^\dagger C_A), \\
G'_A &= \delta_B G_A = \frac{\beta F_\pi^2}{2}(\gamma(C_V \xi_A + \xi_A^\dagger C_V + C_A \xi_V + \xi_V^\dagger C_A + C_V \xi_{M-} - \xi_{M-} C_V - C_A \xi_{M+} - \xi_{M+} C_A) \\
&\quad - (C_V \xi_{M-} - \xi_{M-} C_V - C_A \xi_{M+} - \xi_{M+} C_A)).
\end{aligned} \tag{A.5}$$

By integrating  $B$ ,  $\mathcal{L}_{\text{GF}}$  becomes

$$\begin{aligned}
\mathcal{L}_{\text{GF}} &= -\frac{1}{\alpha_V}\text{tr}[(\partial^\mu V_\mu + \alpha_V(G_V - \frac{1}{N_f}\text{tr}[G_V]))^2] - \frac{1}{\alpha_A}\text{tr}[(\partial^\mu A_\mu + \alpha_A(G_A - \frac{1}{N_f}\text{tr}[G_A]))^2] \\
&= -\frac{1}{\alpha_V}\text{tr}[(\partial^\mu V_\mu)^2] - \frac{1}{\alpha_A}\text{tr}[(\partial^\mu A_\mu)^2] - 2\text{tr}[\partial^\mu V_\mu G_V] - 2\text{tr}[\partial^\mu A_\mu G_A] \\
&\quad - \alpha_V(\text{tr}[G_V^2] - \frac{1}{N_f}\text{tr}[G_V]^2) - \alpha_A(\text{tr}[G_A^2] - \frac{1}{N_f}\text{tr}[G_A]^2),
\end{aligned} \tag{A.6}$$

where  $N_f$  is the number of flavor.

## APPENDIX B: RENORMALIZATION

Counter terms from  $\mathcal{O}(p^4)$  Lagrangian are also necessary to cancel the divergences of one-loop diagrams in addition to counter terms from  $\mathcal{O}(p^2)$  Lagrangian. First, we define the renormalized parameters in the  $\mathcal{O}(p^2)$  Lagrangian denoted with the subscript r as:

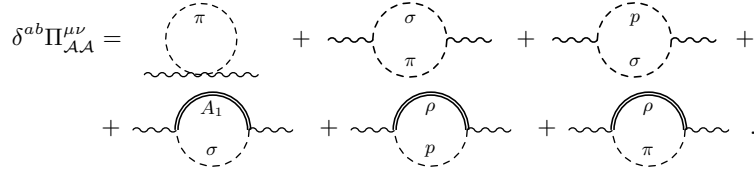
$$\begin{aligned}
\pi &= Z_\pi^{1/2}\pi_r, \quad \sigma = Z_\sigma^{1/2}\sigma_r, \quad p = Z_p^{1/2}p_r + \delta_{\pi p}\pi_r, \\
\rho &= Z_\rho^{1/2}\rho_r, \quad A_1 = Z_{A_1}^{1/2}A_{1r}, \quad g^2 = Z_g g_r^2 \\
F_\pi^2 &= F_{\pi r}^2 + \delta_{F_\pi^2}, \quad F_\sigma^2 = F_{\sigma r}^2 + \delta_{F_\sigma^2}, \quad F_p^2 = F_{pr}^2 + \delta_{F_p^2}, \quad F_{A_1}^2 = F_{A_1 r}^2 + \delta_{F_{A_1}^2},
\end{aligned} \tag{B.1}$$

where  $\delta_{\pi p}$  is necessary to resolve  $\pi$ - $p$  mixing in the loop level. The counter term is defined  $\delta_\phi = 1 - Z_\phi$ , where  $\phi = \pi, p, \rho, A_1, g$ .  $Z_\rho = Z_{A_1}$  or  $\delta_{Z_\rho} = \delta_{Z_{A_1}}$  is satisfied by the parity invariance of the Lagrangian. We explicitly evaluate only the counter terms of  $\mathcal{O}(p^4)$  related to the vector and axial-vector current correlators. The relevant Lagrangian is given by

$$\begin{aligned}
\mathcal{L}_{(4)z} &= \frac{\kappa}{2g^2}\text{tr}[F_{\mu\nu}^{(L)}\xi_M F^{(R)\mu\nu}\xi_M^\dagger] + \frac{z_1 + z_2}{4}\text{tr}[(\mathcal{F}_{\mu\nu}^{(L)})^2 + (\mathcal{F}_{\mu\nu}^{(R)})^2] + \frac{z_1 - z_2}{2}\text{tr}[\mathcal{F}_{\mu\nu}^{(L)}\xi_L^\dagger \xi_M \xi_R \mathcal{F}^{(R)\mu\nu}\xi_R^\dagger \xi_M^\dagger \xi_L] \\
&\quad + \frac{z_3 + z_4}{4}\text{tr}[\xi_L \mathcal{F}_{\mu\nu}^{(L)}\xi_L^\dagger F^{(L)\mu\nu} + \xi_R \mathcal{F}_{\mu\nu}^{(R)}\xi_R^\dagger F^{(R)\mu\nu}] + \frac{z_3 - z_4}{4}\text{tr}[\mathcal{F}_{\mu\nu}^{(L)}\xi_L^\dagger \xi_M F^{(R)\mu\nu}\xi_M^\dagger \xi_L + \mathcal{F}_{\mu\nu}^{(R)}\xi_R^\dagger \xi_M F^{(L)\mu\nu}\xi_M^\dagger \xi_R].
\end{aligned} \tag{B.2}$$

We define renormalized parameters

$$\kappa Z_\rho = \kappa_r + \delta_\kappa, \quad z_{1,2} = z_{r1,2} + \delta_{z_{1,2}}, \quad z_{3,4} Z_\rho^{\frac{1}{2}} Z_g^{\frac{1}{2}} = z_{r3,4} + \delta_{z_{3,4}}. \tag{B.3}$$

FIG. 1: Contributions to  $\Pi_{\mathcal{A}\mathcal{A}}^{\mu\nu}$  at one-loop.

### APPENDIX C: ONE-LOOP CORRECTIONS

In this appendix, we evaluate some two point functions and their divergent part. We define  $A(m^2)$ ,  $B(p, m_1^2, m_2^2)$ ,  $B^\mu(p, m_1^2, m_2^2)$ ,  $B^{\mu\nu}(p, m_1^2, m_2^2)$ ,  $\tilde{B}^{\mu\nu}(p, m_1^2, m_2^2)$  as follows:

$$\begin{aligned}
A(m^2) &= \int \frac{d^4 k}{i(2\pi)^4} \frac{1}{m^2 - k^2}, \\
B(p, m_1^2, m_2^2) &= \int \frac{d^4 k}{i(2\pi)^4} \frac{1}{(m_1^2 - (k-p)^2)(m_2^2 - k^2)}, \\
B^\mu(p, m_1^2, m_2^2) &= \int \frac{d^4 k}{i(2\pi)^4} \frac{k^\mu}{(m_1^2 - (k-p)^2)(m_2^2 - k^2)}, \\
\tilde{B}^{\mu\nu}(p, m_1^2, m_2^2) &= \int \frac{d^4 k}{i(2\pi)^4} \frac{k^\mu k^\nu}{(m_1^2 - (k-p)^2)(m_2^2 - k^2)}, \\
B^{\mu\nu}(p, m_1^2, m_2^2) &= \int \frac{d^4 k}{i(2\pi)^4} \frac{(2k-p)^\mu (2k-p)^\nu}{(m_1^2 - (k-p)^2)(m_2^2 - k^2)}.
\end{aligned} \tag{C.1}$$

The quadratic divergence plays an important role in the Wilsonian renormalization group equations. We identify the poles of  $D = 2$  and  $D = 4$  as the quadratic and logarithmic divergences after employing the dimensional regularization to take into account the quadratic divergence following Refs [35], denoted as:

$$\begin{aligned}
A &\equiv \frac{\Lambda^2}{(4\pi)^2}, \\
B &\equiv \frac{1}{(4\pi)^2} \ln \Lambda^2.
\end{aligned} \tag{C.2}$$

We evaluate the divergent part using  $A$ ,  $B$  as follows

$$\begin{aligned}
A(m^2)|_{\text{div}} &= A - m^2 B, \\
B(p, m_1^2, m_2^2)|_{\text{div}} &= B, \\
B^\mu(p, m_1^2, m_2^2)|_{\text{div}} &= \frac{p^\mu}{2} B, \\
B^{\mu\nu}(p, m_1^2, m_2^2)|_{\text{div}} &= -g^{\mu\nu} (2A - (m_1^2 + m_2^2)B) - P^{\mu\nu} \frac{B}{3}, \\
\tilde{B}^{\mu\nu}(p, m_1^2, m_2^2)|_{\text{div}} &= \frac{1}{4} (B^{\mu\nu} + p^\mu p^\nu B) \\
&= \frac{1}{4} g^{\mu\nu} (-2A + (m_1^2 + m_2^2)B) - P^{\mu\nu} \frac{B}{12} + \frac{1}{4} p^\mu p^\nu B,
\end{aligned} \tag{C.3}$$

where  $P^{\mu\nu} \equiv p^2 g^{\mu\nu} - p^\mu p^\nu$ .

We take the Landau gauge ( $\alpha_V = \alpha_A = 0$ ) in the following calculations of one-loop corrections.

## 1. $\mathcal{A} - \mathcal{A}$

The contributions from each diagram shown in Fig. 1 are

$$(1) : \text{Diagram (1)} = -(1 + \beta\gamma^2 - a)N_f\delta^{ab}g^{\mu\nu}A(0), \quad (\text{C.4})$$

$$(2) : \text{Diagram (2)} = -g^2F_\pi^2(a - \beta\gamma^2)^2N_f\delta^{ab}g^{\mu\nu}B(p, 0, M_\rho^2), \quad (\text{C.5})$$

$$(3) : \text{Diagram (3)} = -g^2F_\pi^2\beta\gamma^2N_f\delta^{ab}g^{\mu\nu}B(p, 0, M_\rho^2), \quad (\text{C.6})$$

$$(4) : \text{Diagram (4)} = -\frac{F_\pi^2}{a}\beta^2\gamma^2g^2N_f\delta^{ab}g^{\mu\nu}B(p, 0, M_{A_1}^2), \quad (\text{C.7})$$

$$(5) : \text{Diagram (5)} = \frac{\beta}{a}\gamma^2N_f\delta^{ab}\tilde{B}^{\mu\nu}(p, 0, 0), \quad (\text{C.8})$$

$$(6) : \text{Diagram (6)} = \frac{1}{a}N_f\delta^{ab}\left[(\beta\gamma^2 - a)^2\tilde{B}^{\mu\nu}(p, 0, 0) - \beta\gamma^2(\beta\gamma^2 - a)(B^\mu(p, 0, 0)p^\nu + p^\mu B^\nu(p, 0, 0))\right. \\ \left. + \beta^2\gamma^4p^\mu p^\nu B(p, 0, 0)\right]. \quad (\text{C.9})$$

With Eq.(C.3) the divergent parts are given by

$$(1) : -N_f\delta^{ab}g^{\mu\nu}(1 + \beta\gamma^2 - a)A, \\ (2) : -N_f\delta^{ab}g^{\mu\nu}g^2F_\pi^2(a - \beta\gamma^2)^2\frac{3}{4}B, \\ (3) : -N_f\delta^{ab}g^{\mu\nu}g^2F_\pi^2\beta\gamma^2\frac{3}{4}B, \\ (4) : -N_f\delta^{ab}g^{\mu\nu}g^2F_\pi^2\frac{\beta^2\gamma^2}{a}\frac{3}{4}B, \\ (5) : \frac{\beta}{a}\gamma^2N_f\delta^{ab}\frac{1}{4}\left(-2g^{\mu\nu}A - P^{\mu\nu}\frac{B}{3} + p^\mu p^\nu B\right), \\ (6) : \frac{1}{a}N_f\delta^{ab}\left((\beta\gamma^2 - a)^2\frac{1}{4}\left(-2g^{\mu\nu}A - P^{\mu\nu}\frac{B}{3}\right) + \frac{1}{4}(\beta\gamma^2 + a)^2p^\mu p^\nu B\right). \quad (\text{C.10})$$

The sum of divergent parts is given by

$$\Pi_{\mathcal{AA}}^{\mu\nu}|_{\text{div}} = N_f\left[g^{\mu\nu}\left(A\left(-(1 + \beta\gamma^2 - a) - \frac{\beta}{2a}\gamma^2 - \frac{1}{2a}(\beta\gamma^2 - a)^2\right) - \frac{3}{4}g^2F_\pi^2B\left((a - \beta\gamma^2)^2 + \beta\gamma^2 + \frac{1}{a}\beta^2\gamma^2\right)\right)\right. \\ \left.- \frac{P^{\mu\nu}}{12}B\left(\frac{\beta}{a}\gamma^2 + \frac{1}{a}(a - \beta\gamma^2)^2\right) + \frac{1}{4}p^\mu p^\nu B\left(\frac{\beta}{a}\gamma^2 + \frac{1}{a}(\beta\gamma^2 + a)^2\right)\right]. \quad (\text{C.11})$$

The divergences can be canceled by the following counterterms:

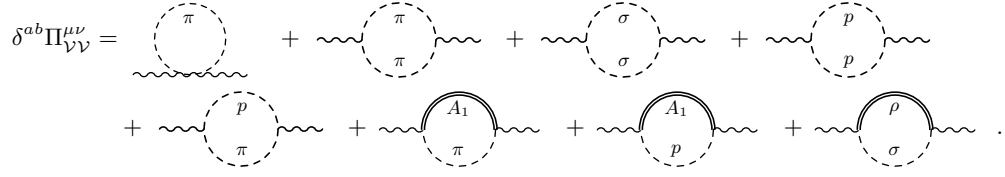
$$\Pi_{\mathcal{AA}}^{\mu\nu}|_{\text{div}} = -(\delta_{F_\pi^2} + \delta_{F_{A_1}^2})g^{\mu\nu} - 2\delta_{Z_2}P^{\mu\nu} + \delta_{\mathcal{AA}}p^\mu p^\nu, \quad (\text{C.12})$$

where we introduce the counterterm  $\delta_{\mathcal{AA}}$  to cancel the divergent part proportional to  $p^\mu p^\nu$ . Such counterterm does not exist in the Lagrangian of any order. This divergence looks accidental. However this divergence is automatically canceled when one calculates an observable such as  $\langle T\mathcal{A}_\mu(x)\mathcal{A}_\nu(0) \rangle$ . Therefore one may simply drop this divergence.

## 2. $\mathcal{V} - \mathcal{V}$

The contributions from each diagram shown in Fig. 2 are

$$(1) : \text{Diagram (1)} = (1 + \beta\gamma^2 - a)N_f\delta^{ab}g^{\mu\nu}A(0), \quad (\text{C.13})$$

FIG. 2: Contributions to  $\Pi_{\mathcal{V}\mathcal{V}}^{\mu\nu}$  at one-loop.

$$(2) : \text{diagram} = \frac{1}{8}(a(1-\gamma^2)-2)^2 N_f \delta^{ab} B^{\mu\nu}(p, 0, 0), \quad (\text{C.14})$$

$$(3) : \text{diagram} = \frac{1}{8} N_f \delta^{ab} B^{\mu\nu}(p, 0, 0), \quad (\text{C.15})$$

$$(4) : \text{diagram} = \frac{a^2}{8\beta^2} N_f \delta^{ab} B^{\mu\nu}(p, 0, 0), \quad (\text{C.16})$$

$$(5) : \text{diagram} = \frac{\gamma^2}{4\beta} N_f \delta^{ab} ((a-\beta)^2 B^{\mu\nu}(p, 0, 0) + p^\mu p^\nu \beta^2 B(p, 0, 0) + 2(a-\beta)\beta(2p^\mu B^\nu(p, 0, 0) - p^\mu p^\nu B(p, 0, 0))), \quad (\text{C.17})$$

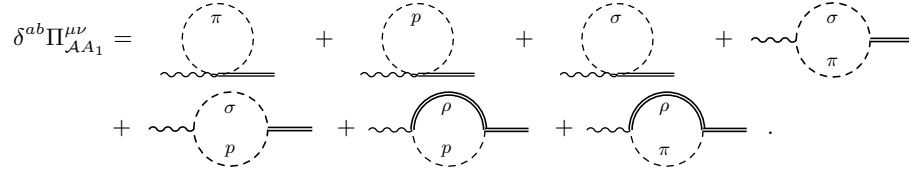
$$(6) : \text{diagram} = -\frac{F_\pi^2 a^2 g^2}{\beta} N_f \delta^{ab} g^{\mu\nu} B(p, 0, M_{A_1}^2), \quad (\text{C.18})$$

$$(7) : \text{diagram} = -F_\pi^2 g^2 \gamma^2 (\beta-a)^2 N_f \delta^{ab} g^{\mu\nu} B(p, 0, M_{A_1}^2), \quad (\text{C.19})$$

$$(8) : \text{diagram} = -a F_\pi^2 g^2 N_f \delta^{ab} g^{\mu\nu} B(p, 0, M_\rho^2). \quad (\text{C.20})$$

The divergent parts are

$$\begin{aligned} (1) : & (1 + \beta\gamma^2 - a) N_f \delta^{ab} g^{\mu\nu} A, \\ (2) : & \frac{1}{8}(a(1-\gamma^2)-2)^2 N_f \delta^{ab} \left( -2g^{\mu\nu} A - P^{\mu\nu} \frac{B}{3} \right), \\ (3) : & \frac{1}{8} N_f \delta^{ab} \left( -2g^{\mu\nu} A - P^{\mu\nu} \frac{B}{3} \right), \\ (4) : & \frac{a^2}{8\beta^2} N_f \delta^{ab} \left( -2g^{\mu\nu} A - P^{\mu\nu} \frac{B}{3} \right), \\ (5) : & \frac{\gamma^2}{4\beta} N_f \delta^{ab} \left( (a-\beta)^2 \left( -2Ag^{\mu\nu} - P^{\mu\nu} \frac{B}{3} \right) + \beta^2 p^\mu p^\nu B \right), \\ (6) : & -\frac{F_\pi^2 a^2 g^2}{\beta} N_f \delta^{ab} g^{\mu\nu} \frac{3}{4} B, \\ (7) : & -F_\pi^2 g^2 \gamma^2 (\beta-a)^2 N_f \delta^{ab} g^{\mu\nu} \frac{3}{4} B, \\ (8) : & -a F_\pi^2 g^2 N_f \delta^{ab} g^{\mu\nu} \frac{3}{4} B. \end{aligned} \quad (\text{C.21})$$

FIG. 3: Contributions to  $\Pi_{AA_1}^{\mu\nu}$  at one-loop.

The sum of divergent parts is given by

$$\begin{aligned} \Pi_{VV}^{\mu\nu}|_{\text{div}} = N_f & \left[ g^{\mu\nu} \left( A \left( (1 + \beta\gamma^2 - a) + \frac{-1}{4}(a(1 - \gamma^2) - 2)^2 - \frac{1}{4} - \frac{a^2}{4\beta^2} - \frac{\gamma^2}{2\beta}(a - \beta)^2 \right) \right. \right. \\ & \left. - \frac{3}{4}F_\pi^2 B \left( \frac{a^2 g^2}{\beta} + g^2 \gamma^2 (\beta - a)^2 + a g^2 \right) \right) \\ & \left. - \frac{P^{\mu\nu}}{24} B((a(1 - \gamma^2) - 2)^2 + 1 + \frac{a^2}{\beta^2} + \frac{2\gamma^2}{\beta}(a - \beta)^2) + p^\mu p^\nu B \frac{\beta\gamma^2}{4} \right]. \end{aligned} \quad (\text{C.22})$$

The divergent part is canceled by following counter terms:

$$\Pi_{VV}^{\mu\nu}|_{\text{div}} = -\delta_{F_\pi^2} g^{\mu\nu} - 2\delta_{z1} P^{\mu\nu}, \quad (\text{C.23})$$

where we drop the divergent term proportional to  $p^\mu p^\nu$ .

### 3. $\mathcal{A} - A_1$

The contributions from each diagram shown in Fig. 3 are

$$(1): \text{Diagram (1)} = \frac{-g\gamma}{2} g^{\mu\nu} (2a - \beta - \beta\gamma^2) N_f \delta^{ab} A(0), \quad (\text{C.24})$$

$$(2): \text{Diagram (2)} = \frac{g\gamma}{2} g^{\mu\nu} N_f \delta^{ab} A(0), \quad (\text{C.25})$$

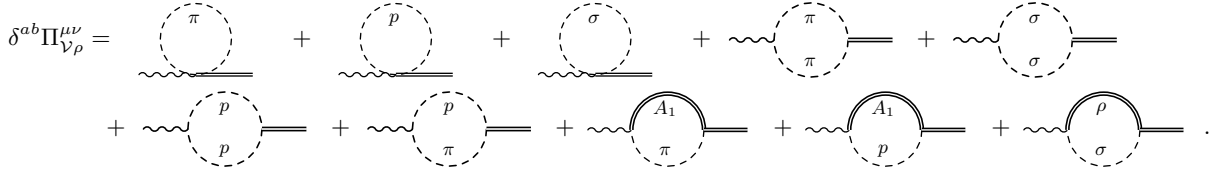
$$(3): \text{Diagram (3)} = \frac{g\gamma}{2} \frac{\beta}{a} g^{\mu\nu} N_f \delta^{ab} A(0), \quad (\text{C.26})$$

$$\begin{aligned} (4): \text{Diagram (4)} &= \frac{g\gamma}{2a} \frac{1}{4} N_f \delta^{ab} \left( 2(a - \beta)(\beta\gamma^2 - a) B^{\mu\nu}(p, 0, 0) - 2(a + \beta\gamma^2)(a - \beta\gamma) p^\mu p^\nu B(p, 0, 0) \right. \\ &\quad \left. + 4(\beta\gamma^2 - a)(a - \beta\gamma) p^\nu B^\mu(p, 0, 0) - 4(a - \beta)(a + \beta\gamma^2) p^\mu B^\nu(p, 0, 0) \right. \\ &\quad \left. - 2((\beta\gamma^2 - a)(a - \beta\gamma) - (a - \beta)(a + \beta\gamma^2)) p^\mu p^\nu B(p, 0, 0) \right), \end{aligned} \quad (\text{C.27})$$

$$\begin{aligned} (5): \text{Diagram (5)} &= \frac{g\gamma}{2a} N_f \delta^{ab} \frac{1}{4} \left( 2a B^{\mu\nu}(p, 0, 0) - 2(a - \beta\gamma) p^\mu p^\nu B(p, 0, 0) \right. \\ &\quad \left. + 4(a - \beta\gamma) p^\nu B^\mu(p, 0, 0) - 4a p^\mu B^\nu(p, 0, 0) + 2\beta\gamma p^\mu p^\nu B(p, 0, 0) \right), \end{aligned} \quad (\text{C.28})$$

$$(6): \text{Diagram (6)} = a F_\pi^2 \gamma (\beta - a) g^2 N_f \delta^{ab} \left( g^{\mu\nu} B(p, 0, M_\rho^2) - \frac{1}{M_\rho^2} \left( \tilde{B}^{\mu\nu}(p, 0, M_\rho^2) - \tilde{B}^{\mu\nu}(p, 0, 0) \right) \right), \quad (\text{C.29})$$

$$(7): \text{Diagram (7)} = -g\gamma F_\pi^2 (a - \beta\gamma^2) (\beta - a) g^2 N_f \delta^{ab} \left( g^{\mu\nu} B(p, 0, M_\rho^2) - \frac{1}{M_\rho^2} \left( \tilde{B}^{\mu\nu}(p, 0, M_\rho^2) - \tilde{B}^{\mu\nu}(p, 0, 0) \right) \right). \quad (\text{C.30})$$

FIG. 4: Contributions to  $\Pi_{\mathcal{V}\rho}^{\mu\nu}$  at one-loop.

The divergent parts are given by

$$\begin{aligned}
(1) &: -\frac{g\gamma}{2}g^{\mu\nu}(2a - \beta - \beta\gamma^2)N_f\delta^{ab}A, \\
(2) &: \frac{g\gamma}{2}g^{\mu\nu}N_f\delta^{ab}A, \\
(3) &: \frac{g\gamma}{2}\frac{\beta}{a}g^{\mu\nu}N_f\delta^{ab}A, \\
(4) &: \frac{g\gamma}{4a}N_f\delta^{ab}\left((a - \beta)(\beta\gamma^2 - a)\left(-2g^{\mu\nu}A - P^{\mu\nu}\frac{B}{3}\right) - (a + \beta\gamma^2)(a - \beta\gamma)p^\mu p^\nu B\right), \\
(5) &: \frac{g\gamma}{2a}N_f\delta^{ab}\frac{1}{4}\left(2a\left(-2g^{\mu\nu}A - P^{\mu\nu}\frac{B}{3}\right) - 2(a - \beta\gamma)p^\mu p^\nu B\right), \\
(6) &: gF_\pi^2\gamma(\beta - a)g^2g^{\mu\nu}N_f\delta^{ab}B\frac{3}{4}, \\
(7) &: -g\gamma F_\pi^2(a - \beta\gamma^2)(\beta - a)g^2g^{\mu\nu}N_f\delta^{ab}B\frac{3}{4}.
\end{aligned} \tag{C.31}$$

The sum of divergent parts is

$$\begin{aligned}
\Pi_{\mathcal{A}A_1}^{\mu\nu}|_{\text{div}} &= N_fg\gamma\left[g_{\mu\nu}\left(\frac{A}{2}\left(-(2a - \beta - \beta\gamma^2) + 1 + \frac{\beta}{a} - \frac{1}{a}(a - \beta)(\beta\gamma^2 - a) - 1\right)\right.\right. \\
&\quad \left.+ B\frac{3}{4}F_\pi^2g^2((\beta - a) - (a - \beta\gamma^2)(\beta - a))\right) \\
&\quad \left.- P^{\mu\nu}\frac{B}{12}\left(\frac{1}{a}(a - \beta)(\beta\gamma^2 - a) + 1\right) - p^\mu p^\nu B\frac{1}{4a}(a - \beta\gamma)(a + \beta\gamma^2 + 1)\right].
\end{aligned} \tag{C.32}$$

The divergences are canceled out by the following counterterms:

$$\Pi_{\mathcal{A}A_1}^{\mu\nu}|_{\text{div}} = g^{\mu\nu}\frac{gF_pF_{A_1}}{2}\left(\frac{\delta F_{A_1}^2}{F_{A_1}^2} + \delta_{ZA_1}\frac{\delta F_p^2}{F_p^2} + \delta_{Z_g}\right) - 2g\delta_{z_4}P^{\mu\nu}. \tag{C.33}$$

where we drop the divergent term proportional to  $p^\mu p^\nu$ .

#### 4. $\mathcal{V} - \rho$

The contributions from each diagram shown in Fig. 4 are

$$(1) : \text{Diagram (1)} = -\frac{1}{2}g(2\beta\gamma^2 - a\gamma^2 - a)N_f\delta^{ab}g^{\mu\nu}A(0), \tag{C.34}$$

$$(2) : \text{Diagram (2)} = \frac{1}{2}g\frac{a}{\beta}N_f\delta^{ab}g^{\mu\nu}A(0), \tag{C.35}$$

$$(3) : \text{Diagram (3)} = \frac{1}{2}gN_f\delta^{ab}g^{\mu\nu}A(0), \tag{C.36}$$



$$(4) : \text{diagram} = \frac{1}{8}ag(1-\gamma^2)(2-a(1-\gamma^2))N_f\delta^{ab}B^{\mu\nu}(p,0,0), \quad (\text{C.37})$$

$$(5) : \text{diagram} = \frac{1}{8}gN_f\delta^{ab}B^{\mu\nu}(p,0,0), \quad (\text{C.38})$$

$$(6) : \text{diagram} = \frac{(2\beta-a)}{8\beta^2}agN_f\delta^{ab}B^{\mu\nu}(p,0,0), \quad (\text{C.39})$$

$$(7) : \text{diagram} = \frac{-\gamma g}{4\beta}N_f\delta^{ab}(\gamma(a-\beta)^2B^{\mu\nu}(p,0,0) - \beta(a-\beta\gamma)p^\mu p^\nu B(p,0,0) \\ - 2\beta\gamma(a-\beta)p^\mu B^\nu + 2(a-\beta)(a-\beta\gamma)p^\nu B^\mu - (a-\beta)(a-2\beta\gamma)p^\mu p^\nu B), \quad (\text{C.40})$$

$$(8) : \text{diagram} = F_\pi^2 g^3 \gamma^2 (\beta-a)^2 N_f \delta^{ab} \left( g^{\mu\nu} B(p,0,M_{A_1}^2) - \frac{1}{M_{A_1}^2} \left( \tilde{B}^{\mu\nu}(p,0,M_{A_1}^2) - \tilde{B}^{\mu\nu}(p,0,0) \right) \right), \quad (\text{C.41})$$

$$(9) : \text{diagram} = -F_\pi^2 g^3 \frac{a}{\beta} (\beta-a) N_f \delta^{ab} \left( g^{\mu\nu} B(p,0,M_{A_1}^2) - \frac{1}{M_{A_1}^2} \left( \tilde{B}^{\mu\nu}(p,0,M_{A_1}^2) - \tilde{B}^{\mu\nu}(p,0,0) \right) \right), \quad (\text{C.42})$$

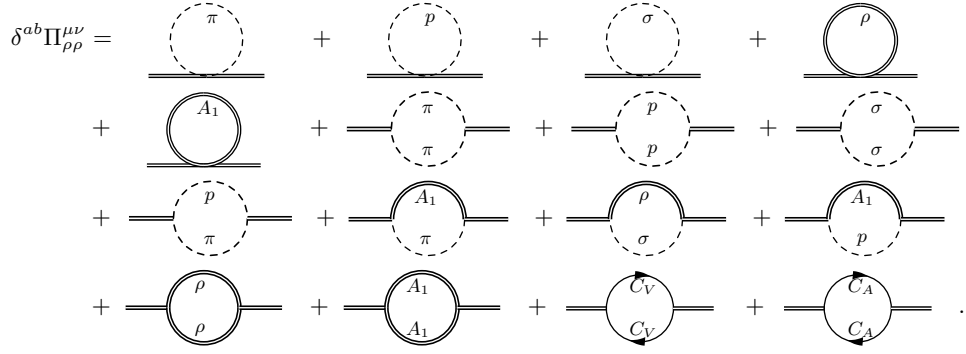
$$(10) : \text{diagram} = 0. \quad (\text{C.43})$$

The divergent parts are given by

$$(1) : -\frac{1}{2}g(2\beta\gamma^2 - a\gamma^2 - a)N_f\delta^{ab}g^{\mu\nu}A, \\ (2) : \frac{1}{2}g\frac{a}{\beta}N_f\delta^{ab}g^{\mu\nu}A, \\ (3) : \frac{1}{2}gN_f\delta^{ab}g^{\mu\nu}A, \\ (4) : \frac{1}{8}ag(1-\gamma^2)(2-a(1-\gamma^2))N_f\delta^{ab} \left( -2g^{\mu\nu}A - P^{\mu\nu}\frac{B}{3} \right), \\ (5) : \frac{1}{8}gN_f\delta^{ab} \left( -2g^{\mu\nu}A - P^{\mu\nu}\frac{B}{3} \right), \\ (6) : \frac{(2\beta-a)}{8\beta^2}agN_f\delta^{ab} \left( -2g^{\mu\nu}A - P^{\mu\nu}\frac{B}{3} \right), \\ (7) : \frac{-\gamma g}{4\beta}N_f\delta^{ab} \left( \gamma(a-\beta)^2 \left( -2g^{\mu\nu}A - P^{\mu\nu}\frac{B}{3} \right) + \beta(\beta\gamma-a)p^\mu p^\nu B \right), \\ (8) : gN_f\delta^{ab}g^{\mu\nu}\gamma^2(\beta-a)^2\frac{3}{4}F_\pi^2g^2B, \\ (9) : -g\frac{a}{\beta}(\beta-a)N_f\delta^{ab}F_\pi^2g^2\frac{3}{4}B, \\ (10) : 0. \quad (\text{C.44})$$

The sum of divergent parts is given by

$$\Pi_{V\rho}^{\mu\nu} = gN_f \left[ g^{\mu\nu} \left( A \left( \frac{1}{2} - \beta\gamma^2 + \frac{1}{2}a\gamma^2 + \frac{1}{2}a + \frac{a}{2\beta} + \frac{-1}{4}a(1-\gamma^2)(2-a(1-\gamma^2)) \right) \right. \right. \\ \left. \left. - \frac{1}{4} - \frac{(2\beta-a)}{4\beta^2}a + \frac{\gamma^2}{2\beta}(a-\beta)^2 \right) + \frac{3}{4}F_\pi^2g^2B \left( \gamma^2(\beta-a)^2 - \frac{a}{\beta}(\beta-a) \right) \right) \\ \left. - P^{\mu\nu}\frac{B}{24} \left( a(1-\gamma^2)(2-a(1-\gamma^2)) + 1 + \frac{(2\beta-a)}{\beta^2}a + \frac{-2\gamma^2}{\beta}(a-\beta)^2 \right) - p^\mu p^\nu B\frac{\gamma}{4}(\beta\gamma-a) \right]. \quad (\text{C.45})$$

FIG. 5: Contributions to  $\Pi_{\rho\rho}^{\mu\nu}$  at one-loop.

The divergence is canceled by the following counterterms:

$$\Pi_{V\rho}^{\mu\nu}\Big|_{\text{div}} = \frac{F_\sigma^2 g}{2} \left( 2 \frac{\delta F_\sigma^2}{F_\sigma^2} + \delta Z_g + \delta Z_\rho \right) g^{\mu\nu} - 2g \delta Z_4 P^{\mu\nu}. \quad (\text{C.46})$$

where we drop the divergent term proportional to  $p^\mu p^\nu$ .

### 5. $\rho - \rho$

The contributions from each diagram shown in Fig. 5 are

$$(1) : \text{tadpole}(\pi) = -g^2(a - \beta)\gamma^2 N_f \delta^{ab} g^{\mu\nu} A(0), \quad (\text{C.47})$$

$$(2) : \text{tadpole}(p) = \frac{-g^2}{\beta}(a - \beta) N_f \delta^{ab} g^{\mu\nu} A(0), \quad (\text{C.48})$$

$$(3) : \text{tadpole}(\sigma) = 0, \quad (\text{C.49})$$

$$(4) : \text{tadpole}(\rho) = g^2 N_f \delta^{ab} g^{\mu\nu} \frac{(D-1)^2}{D} A(M_\rho^2), \quad (\text{C.50})$$

$$(5) : \text{tadpole}(A_1) = g^2 N_f \delta^{ab} g^{\mu\nu} \frac{(D-1)^2}{D} A(M_{A_1}^2), \quad (\text{C.51})$$

$$(6) : \text{bubble}(\pi) = \frac{1}{8} a^2 g^2 (1 - \gamma^2)^2 N_f \delta^{ab} B^{\mu\nu}(p, 0, 0), \quad (\text{C.52})$$

$$(7) : \text{bubble}(p) = \frac{1}{8\beta^2} (2\beta - a)^2 g^2 N_f \delta^{ab} B^{\mu\nu}(p, 0, 0), \quad (\text{C.53})$$

$$(8) : \text{bubble}(\sigma) = \frac{1}{8} g^2 B^{\mu\nu}(p, 0, 0), \quad (\text{C.54})$$

$$(9) : \text{bubble}(\pi) = \frac{1}{4\beta} g^2 N_f \delta^{ab} (\gamma^2 (a - \beta)^2 B^{\mu\nu}(p, 0, 0) + (\beta\gamma - a)^2 p^\mu p^\nu B(p, 0, 0) + 2\gamma(\beta - a)(\beta\gamma - a)(p^\mu B^\nu(p, 0, 0) + p^\nu B^\mu(p, 0, 0) - p^\mu p^\nu B(p, 0, 0))), \quad (\text{C.55})$$

$$(10): \quad \text{Diagram} = -F_\pi^2(\beta - a)^2 \gamma^2 g^4 N_f \delta^{ab} \left( g^{\mu\nu} B(p, 0, M_{A_1}^2) - \frac{1}{M_{A_1}^2} \left( \tilde{B}^{\mu\nu}(p, 0, M_{A_1}^2) - \tilde{B}^{\mu\nu}(p, 0, 0) \right) \right), \quad (\text{C.56})$$

$$(11): \text{Diagram with a solid upper arc labeled } \rho \text{ and a dashed lower arc labeled } \sigma = 0, \quad (\text{C.57})$$

$$(12) : \text{Diagram} = -\frac{F_\pi^2}{\beta}(\beta - a)^2 g^4 N_f \delta^{ab} \left( g^{\mu\nu} B(p, 0, M_{A_1}^2) - \frac{1}{M_{A_1}^2} \left( \tilde{B}^{\mu\nu}(p, 0, M_{A_1}^2) - \tilde{B}^{\mu\nu}(p, 0, 0) \right) \right), \quad (\text{C.58})$$

$$\begin{aligned}
(13) : \quad \text{---} \bigcirc \text{---} &= \frac{1}{2} g^2 N_f \delta^{ab} \int \frac{d^4 k}{i(2\pi)^4} \frac{1}{((k-p)^2 - M_\rho^2)(k^2 - M_\rho^2)} \\
&\times \{-2p^\rho g^{\mu\sigma} + 2p^\sigma g^{\mu\rho} + (p-2k)^\mu g^{\rho\sigma}\} \{-2p^{\rho'} g^{\nu\sigma'} + 2p^{\sigma'} g^{\nu\rho'} + (p-2k)^\nu g^{\rho'\sigma'}\} \\
&\times (g_{\rho\rho'} - \frac{k_\rho k_{\rho'}}{k^2})(g_{\sigma\sigma'} - \frac{(k-p)_\sigma (k-p)_{\sigma'}}{(k-p)^2}), \tag{C.59}
\end{aligned}$$

$$\begin{aligned}
(14) : \quad \text{---} \bigcirc_{A_1} \text{---} &= \frac{1}{2} g^2 N_f \delta^{ab} \int \frac{d^4 k}{i(2\pi)^4} \frac{1}{((k-p)^2 - M_{A_1}^2)(k^2 - M_{A_1}^2)} \\
&\times \{ -2p^\rho g^{\mu\sigma} + 2p^\sigma g^{\mu\rho} + (p-2k)^\mu g^{\rho\sigma} \} \{ -2p^{\rho'} g^{\nu\sigma'} + 2p^{\sigma'} g^{\nu\rho'} + (p-2k)^\nu g^{\rho'\sigma'} \} \\
&\times (g_{\rho\rho'} - \frac{k_\rho k_{\rho'}}{k^2})(g_{\sigma\sigma'} - \frac{(k-p)_\sigma (k-p)_{\sigma'}}{(k-p)^2}), \tag{C.60}
\end{aligned}$$

$$(15) : \text{Diagram} = \frac{-g^2}{4} N_f \delta^{ab} (B^{\mu\nu}(p, 0, 0) - p^\mu p^\nu B(p, 0, 0)), \quad (\text{C.61})$$

$$(16) : \text{Diagram} = \frac{-g^2}{4} N_f \delta^{ab} (B^{\mu\nu}(p, 0, 0) - p^\mu p^\nu B(p, 0, 0)), \quad (\text{C.62})$$

where  $D$  is the space-time dimension. To keep the gauge invariance we take  $D \rightarrow 4$  after the sum of diagram. The divergent parts are given by

$$\begin{aligned}
(1) : & -g^2(a-\beta)\gamma^2 N_f \delta^{ab} g^{\mu\nu} A, \\
(2) : & \frac{-g^2}{\beta}(a-\beta) N_f \delta^{ab} g^{\mu\nu} A, \\
(3) : & 0, \\
(4) : & g^2 N_f \delta^{ab} g^{\mu\nu} \frac{(D-1)^2}{D} A(M_\rho^2), \\
(5) : & g^2 N_f \delta^{ab} g^{\mu\nu} \frac{(D-1)^2}{D} A(M_{A_1}^2), \\
(6) : & \frac{1}{8} a^2 g^2 (1-\gamma^2)^2 N_f \delta^{ab} \left( -2g^{\mu\nu} A - P^{\mu\nu} \frac{B}{3} \right), \\
(7) : & \frac{1}{8\beta^2} (2\beta-a)^2 g^2 N_f \delta^{ab} \left( -2g^{\mu\nu} A - P^{\mu\nu} \frac{B}{3} \right), \\
(8) : & \frac{1}{8} g^2 N_f \delta^{ab} \left( -2g^{\mu\nu} A - P^{\mu\nu} \frac{B}{3} \right), \\
(9) : & \frac{1}{4\beta} g^2 N_f \delta^{ab} \left( g^{\mu\nu} (-2\gamma^2(a-\beta)^2 A + (\beta\gamma-a)^2 p^2 B) - P^{\mu\nu} \left( \frac{\gamma^2(a-\beta)^2}{3} + (\beta\gamma-a)^2 \right) B \right), \\
(10) : & -F_\pi^2 (\beta-a)^2 \gamma^2 g^2 N_f \delta^{ab} g^{\mu\nu} \frac{3}{4} B, \\
(11) : & 0,
\end{aligned}$$

$$\begin{aligned}
(12) : & -\frac{F_\pi^2}{\beta}(\beta - a)^2 g^2 g^2 N_f \delta^{ab} g^{\mu\nu} \frac{3}{4} B, \\
(13) : & \frac{1}{2} g^2 N_f \delta^{ab} \left( P^{\mu\nu} \frac{14}{3} B - 2(D-1) g^{\mu\nu} A(M_\rho^2) - \frac{p^2 g^{\mu\nu}}{2} B \right), \\
(14) : & \frac{1}{2} g^2 N_f \delta^{ab} \left( P^{\mu\nu} \frac{14}{3} B - 2(D-1) g^{\mu\nu} A_{M_{A_1}^2} - \frac{p^2 g^{\mu\nu}}{2} B \right), \\
(15) : & -\frac{g^2}{4} N_f \delta^{ab} \left( -g^{\mu\nu} (2A + p^2 B) + P^{\mu\nu} \frac{2B}{3} \right), \\
(16) : & -\frac{g^2}{4} N_f \delta^{ab} \left( -g^{\mu\nu} (2A + p^2 B) + P^{\mu\nu} \frac{2B}{3} \right). \tag{C.63}
\end{aligned}$$

The divergent part including the internal line of  $\rho$  is given by

$$\begin{aligned}
(4) + (13) + (15) &= g^2 N_f \delta^{ab} \left[ g^{\mu\nu} \left( \frac{(D-1)^2}{D} A(M_\rho^2) - (D-1) A(M_\rho^2) - \frac{p^2}{4} B + \frac{1}{4} (2A + p^2 B) \right) \right. \\
&\quad \left. + P^{\mu\nu} \left( \frac{7}{3} B - \frac{1}{4} \frac{2B}{3} \right) \right] \\
&= g^2 N_f \delta^{ab} \left[ g^{\mu\nu} \left( \frac{1}{D} (1 - \frac{1}{2} D) A(M_\rho^2) - \frac{1}{2} A(M_\rho^2) + \frac{1}{2} A \right) + P^{\mu\nu} \frac{13}{6} B \right] \\
&= g^2 N_f \delta^{ab} \left[ g^{\mu\nu} \frac{3}{4} M_\rho^2 B + P^{\mu\nu} \frac{13}{6} B \right], \tag{C.64}
\end{aligned}$$

where we take  $D \rightarrow 4$  and use

$$\lim_{D \rightarrow 4} \frac{1}{D} (1 - \frac{1}{2} D) A(M_\rho^2) = \frac{1}{4} M_\rho^2 B. \tag{C.65}$$

Similarly the divergent part including the internal line of  $A_1$  is

$$(5) + (14) + (16) = g^2 N_f \delta^{ab} \left[ g^{\mu\nu} \frac{3}{4} M_{A_1}^2 B + P^{\mu\nu} \frac{13}{6} B \right]. \tag{C.66}$$

The sum of divergent part is given by

$$\begin{aligned}
\Pi_{\rho\rho}^{\mu\nu}|_{\text{div}} &= g^2 N_f \delta^{ab} \left[ g^{\mu\nu} \left( A \left( -(a-\beta)\gamma^2 + \frac{-1}{\beta}(a-\beta) - \frac{1}{4} a^2 (1-\gamma^2)^2 - \frac{1}{4\beta^2} (2\beta-a)^2 - \frac{1}{4} + \frac{-\gamma^2(a-\beta)^2}{2\beta} \right) \right. \right. \\
&\quad \left. \left. - F_\pi^2 g^2 \frac{3}{4} B \left( (\beta-a)^2 \frac{1}{\beta} (\beta\gamma^2 + 1) - (a+\beta) \right) \right) \right. \\
&\quad \left. + P^{\mu\nu} B \left( \frac{13}{3} + \frac{1}{24} \left( -a^2 (1-\gamma^2)^2 - \frac{1}{\beta^2} (2\beta-a)^2 - 1 - \frac{2\gamma^2(a-\beta)^2}{\beta} - \frac{6}{\beta} (\beta\gamma-a)^2 \right) \right) \right]. \tag{C.67}
\end{aligned}$$

The divergent part is canceled out by the following counterterms:

$$\Pi_{\rho\rho}^{\mu\nu}|_{\text{div}} = -(M_\rho^2 (\delta_{Z_g} + \delta_{Z_\rho}) + g^2 \delta_{F_\pi^2}) g^{\mu\nu} + (\delta_{Z_\rho} + 2\delta_\kappa) P^{\mu\nu}. \tag{C.68}$$

## 6. $A_1 - A_1$

The contributions from each diagram shown in Fig. 6 are

$$(1) : \quad \text{Diagram with a dashed circle labeled } \pi \text{ above it, connected to two horizontal lines.} \quad = g^2 (a-\beta) \gamma^2 N_f \delta^{ab} g^{\mu\nu} A(0), \tag{C.69}$$

$$(2) : \quad \text{Diagram with a dashed circle labeled } p \text{ above it, connected to two horizontal lines.} \quad = \frac{g^2}{\beta} (a-\beta) N_f \delta^{ab} g^{\mu\nu} A(0), \tag{C.70}$$

$$\Pi_{A_1 A_1}^{\mu\nu} = \text{[12 diagrams]} .$$

FIG. 6: Contributions to  $\Pi_{A_1 A_1}^{\mu\nu}$  at one-loop.

$$(3) : \text{[diagram]} = 0, \quad (C.71)$$

$$(4) : \text{[diagram]} = g^2 N_f \delta^{ab} g^{\mu\nu} \frac{(D-1)^2}{D} A(M_\rho^2), \quad (C.72)$$

$$(5) : \text{[diagram]} = g^2 N_f \delta^{ab} g^{\mu\nu} \frac{(D-1)^2}{D} A(M_{A_1}^2), \quad (C.73)$$

$$(6) : \text{[diagram]} = \frac{g^2 \gamma^2}{4a} N_f \delta^{ab} ((a-\beta)^2 B^{\mu\nu}(p, 0, 0) + (\beta\gamma - a)^2 p^\mu p^\nu B(p, 0, 0) + 2(\beta - a)(\beta\gamma - a)(p^\mu B^\nu(p, 0, 0) + p^\nu B^\mu(p, 0, 0) - p^\mu p^\nu B(p, 0, 0))), \quad (C.74)$$

$$(7) : \text{[diagram]} = \frac{g^2}{4a\beta} N_f \delta^{ab} (a^2 B^{\mu\nu}(p, 0, 0) + (\beta\gamma - a)^2 p^\mu p^\nu B(p, 0, 0) + 2a(a - \beta\gamma)(p^\mu B^\nu(p, 0, 0) + p^\nu B^\mu(p, 0, 0) - p^\mu p^\nu B(p, 0, 0))), \quad (C.75)$$

$$(8) : \text{[diagram]} = 0, \quad (C.76)$$

$$(9) : \text{[diagram]} = -F_\pi^2 (\beta - a)^2 \gamma^2 g^4 N_f \delta^{ab} \left( g^{\mu\nu} B(p, 0, M_\rho^2) - \frac{1}{M_\rho^2} \left( \tilde{B}^{\mu\nu}(p, 0, M_\rho^2) - \tilde{B}^{\mu\nu}(p, 0, 0) \right) \right), \quad (C.77)$$

$$(10) : \text{[diagram]} = -\frac{F_\pi^2}{\beta} (\beta - a)^2 g^4 N_f \delta^{ab} \left( g^{\mu\nu} B(p, 0, M_\rho^2) - \frac{1}{M_\rho^2} \left( \tilde{B}^{\mu\nu}(p, 0, M_\rho^2) - \tilde{B}^{\mu\nu}(p, 0, 0) \right) \right), \quad (C.78)$$

$$(11) : \text{[diagram]} = g^2 N_f \delta^{ab} \int \frac{d^4 k}{i(2\pi)^4} \frac{1}{((k-p)^2 - M_\rho^2)(k^2 - M_{A_1}^2)} \times \{ -2p^\rho g^{\mu\sigma} + 2p^\sigma g^{\mu\rho} + (p-2k)^\mu g^{\rho\sigma} \} \{ -2p^{\rho'} g^{\nu\sigma'} + 2p^{\sigma'} g^{\nu\rho'} + (p-2k)^\nu g^{\rho'\sigma'} \} \times (g_{\rho\rho'} - \frac{k_\rho k_{\rho'}}{k^2})(g_{\sigma\sigma'} - \frac{(k-p)_\sigma (k-p)_{\sigma'}}{(k-p)^2}), \quad (C.79)$$

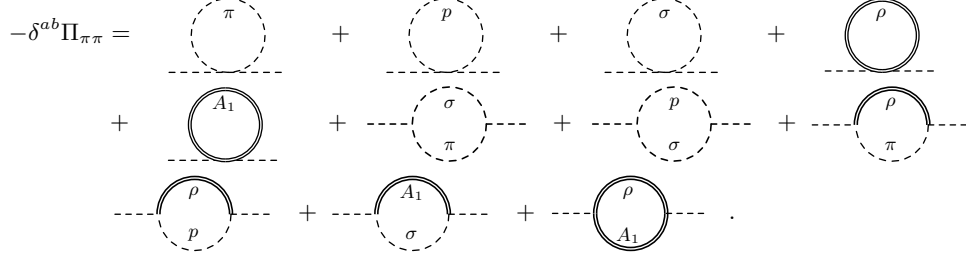
$$(12) : \text{[diagram]} = \frac{-g^2}{2} N_f \delta^{ab} (B^{\mu\nu}(p, 0, 0) - p^\mu p^\nu B(p, 0, 0)). \quad (C.80)$$

The divergent parts are given by

$$(1) : g^2 (a - \beta) \gamma^2 N_f \delta^{ab} g^{\mu\nu} A,$$

$$(2) : \frac{g^2}{\beta} (a - \beta) N_f \delta^{ab} g^{\mu\nu} A,$$

$$(3) : 0,$$

FIG. 7: Contributions to  $\Pi_{\pi\pi}$  at one-loop.

$$\begin{aligned}
(4) : & g^2 N_f \delta^{ab} g^{\mu\nu} \frac{(D-1)^2}{D} (A - M_\rho^2 B), \\
(5) : & g^2 N_f \delta^{ab} g^{\mu\nu} \frac{(D-1)^2}{D} (A - M_{A_1}^2 B), \\
(6) : & \frac{g^2 \gamma^2}{4a} N_f \delta^{ab} \left( -2g^{\mu\nu} (a-\beta)^2 A - P^{\mu\nu} \frac{1}{3} (a-\beta)^2 B + (\beta\gamma - a)^2 p^\mu p^\nu B \right), \\
(7) : & \frac{g^2}{4a\beta} N_f \delta^{ab} \left( -2a^2 A g^{\mu\nu} - P^{\mu\nu} \frac{a^2}{3} B + (\beta\gamma - a)^2 p^\mu p^\nu \right), \\
(8) : & 0, \\
(9) : & -N_f \delta^{ab} F_\pi^2 (\beta - a)^2 \gamma^2 g^{\mu\nu} \frac{D-1}{D} B, \\
(10) : & -N_f \delta^{ab} \frac{F_\pi^2}{\beta} (\beta - a)^2 g^{\mu\nu} \frac{D-1}{D} B, \\
(11) : & N_f \delta^{ab} g^2 \left( P^{\mu\nu} \frac{14}{3} B - 2g^{\mu\nu} A + 3g^{\mu\nu} (M_\rho^2 + M_{A_1}^2) B - \frac{g^{\mu\nu} p^2}{2} B \right), \\
(12) : & -\frac{g^2}{2} N_f \delta^{ab} \left( -g^{\mu\nu} (2A + p^2 B) + P^{\mu\nu} \frac{2B}{3} \right). \tag{C.81}
\end{aligned}$$

$$(4) + (5) + (11) + (12) = g^2 N_f \delta^{ab} \left[ g^{\mu\nu} \frac{3}{4} (M_\rho^2 + M_{A_1}^2) B + P^{\mu\nu} \frac{13}{3} B \right]. \tag{C.82}$$

The sum of divergent parts is given by

$$\begin{aligned}
\Pi_{A_1 A_1}^{\mu\nu} |_{\text{div}} = & g^2 N_f \delta^{ab} \left[ g^{\mu\nu} \left( A \left( (a-\beta)\gamma^2 + \frac{1}{\beta}(a-\beta) - \frac{\gamma^2}{2a}(a-\beta)^2 - \frac{a}{2\beta} \right) \right. \right. \\
& \left. \left. - \frac{3}{4} F_\pi^2 g^2 B ((\beta-a)^2 \gamma^2 + \frac{1}{\beta}(\beta-a)^2 - (a+\beta)) \right) \right. \\
& \left. + P^{\mu\nu} B \left( \frac{13}{3} - \frac{1}{12} \frac{\gamma^2}{a} (a-\beta)^2 + 3 \frac{\gamma^2}{a} (\beta\gamma - a)^2 + \frac{1}{a\beta} a^2 + 3 \frac{1}{a\beta} (\beta\gamma - a)^2 \right) \right]. \tag{C.83}
\end{aligned}$$

The divergent part is canceled out by the following counterterms:

$$\Pi_{A_1 A_1}^{\mu\nu} |_{\text{div}} = -(M_{A_1}^2 (\delta_{Z_g} + \delta_{Z_{A_1}}) + g^2 \delta_{F_p^2}) g^{\mu\nu} + (\delta_{Z_\rho} - 2\delta_\kappa) P^{\mu\nu}. \tag{C.84}$$

7.  $\pi - \pi$ 

The contributions from each diagram shown in Fig. 7 are

$$(1): \quad \text{Diagram: a dashed circle with a dashed line below it} \quad = -\frac{4-3a(1-\gamma^2)^2}{12} \frac{p^2}{F_\pi^2} N_f \delta^{ab} A(0), \quad (\text{C.85})$$

$$(2): \quad \text{Diagram: a dashed circle with a horizontal dashed line passing through its center, labeled } \sigma \text{ above it.} \quad = \frac{\beta\gamma^2}{a} \frac{p^2}{F_\pi^2} N_f \delta^{ab} A(0), \quad (\text{C.86})$$

$$(3) : \quad \text{Diagram: a dashed circle with a dashed line segment below it} = \frac{a\gamma^2}{4\beta} \frac{p^2}{F_\pi^2} N_f \delta^{ab} A(0), \quad (\text{C.87})$$

$$(4): \quad \text{Diagram: A circle with radius } \rho \text{ and a dashed line below it.} \quad = -g^2(a - \beta)\gamma^2 N_f \delta^{ab}(1 - D)A(M_\rho^2), \quad (\text{C.88})$$

$$(5): \quad \text{Diagram: a circle with } A_1 \text{ inside, connected to a dashed line below it} \quad = g^2(a - \beta)\gamma^2\delta^{ab}N_f(1 - D)A(M_{A_1}^2), \quad (\text{C.89})$$

$$(6): \quad \text{---} \circ \text{---} = \frac{a(1-\gamma^2)^2}{4} \frac{p^2}{F_\pi^2} N_f \delta^{ab} (A(0) + p^2 B(p, 0, 0)), \quad (\text{C.90})$$

$$(7) : \text{---} \circ_{\sigma}^p \text{---} = \frac{\gamma^2}{4a\beta} \frac{p^2}{F_\pi^2} N_f \delta^{ab} ((-4\beta a - 2\beta^2 + a^2)A(0) + (\beta - a)^2 p^2 B(p, 0, 0)), \quad (\text{C.91})$$

$$(8) : \text{---}\text{---}\text{---} \circlearrowleft^{\rho}_{\pi} \text{---}\text{---}\text{---} = -g^2 a^2 (1-\gamma^2)^2 N_f \delta^{ab} \left( p^2 B(p, 0, M_\rho^2) - \frac{p^\mu p^\nu}{M_\rho^2} \left( \tilde{B}_{\mu\nu}(p, 0, M_\rho^2) - \tilde{B}_{\mu\nu}(p, 0, 0) \right) \right), \quad (\text{C.92})$$

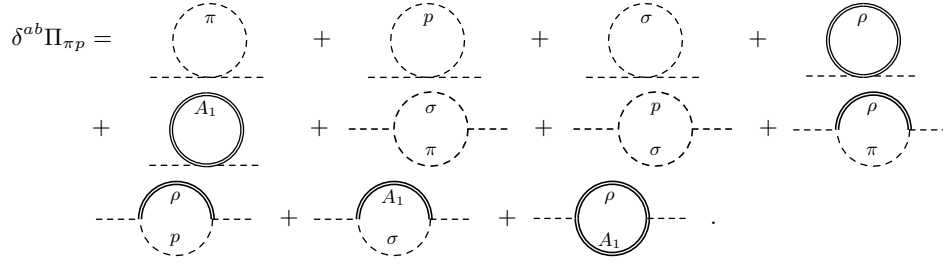
$$(9) : \text{---}\text{---}\text{---} \circlearrowleft^{\rho} \text{---}\text{---}\text{---} = \frac{-1}{\beta} g^2 (a - \beta)^2 \gamma^2 N_f \delta^{ab} \left( p^2 B(p, 0, M_\rho^2) - \frac{p^\mu p^\nu}{M_\rho^2} \left( \tilde{B}_{\mu\nu}(p, 0, M_\rho^2) - \tilde{B}_{\mu\nu}(p, 0, 0) \right) \right), \quad (\text{C.93})$$

$$(10) : \text{---} \bigcirc \text{---} = \frac{-\gamma^2}{a} g^2 (\beta - a)^2 N_f \delta^{ab} \left( p^2 B(p, 0, M_{A_1}^2) - \frac{p^\mu p^\nu}{M_{A_1}^2} \left( \tilde{B}_{\mu\nu}(p, 0, M_{A_1}^2) - \tilde{B}_{\mu\nu}(p, 0, 0) \right) \right), \quad (\text{C.94})$$

$$\begin{aligned}
(11) : \quad \text{---} \circlearrowleft_{A_1}^{\rho} \text{---} &= F_\pi^2 g^4 (\beta - a)^2 \gamma^2 N_f \delta^{ab} \left( (D-1) B(p, M_\rho^2, M_{A_1}^2) - \frac{p^2}{M_{A_1}^2} (B(p, M_{A_1}^2, M_\rho^2) - B(p, 0, M_\rho^2)) \right. \\
&\quad \left. + \frac{p^\mu p^\nu}{M_{A_1}^2 M_\rho^2} (\tilde{B}_{\mu\nu}(p, M_{A_1}^2, M_\rho^2) - \tilde{B}_{\mu\nu}(p, 0, M_\rho^2)) \right). \quad (C.95)
\end{aligned}$$

The divergent parts are give by

$$\begin{aligned}
(1) : & -\frac{4-3a(1-\gamma^2)^2}{12}\frac{p^2}{F_\pi^2}N_f\delta^{ab}A, \\
(2) : & \frac{\beta\gamma^2}{a}\frac{p^2}{F_\pi^2}N_f\delta^{ab}A, \\
(3) : & \frac{\gamma^2}{\beta}\frac{1}{4}a\frac{p^2}{F_\pi^2}N_f\delta^{ab}A, \\
(4) : & g^2(a-\beta)\gamma^2N_f\delta^{ab}(D-1)(A-M_\rho^2B), \\
(5) : & -g^2(a-\beta)\gamma^2N_f\delta^{ab}(D-1)(A-M_{A_1}^2B), \\
(6) : & \frac{a(1-\gamma^2)^2}{4}\frac{p^2}{F_\pi^2}N_f\delta^{ab}(A+p^2B), \\
(7) : & \frac{\gamma^2}{4a\beta}\frac{p^2}{F_\pi^2}N_f\delta^{ab}((a^2-2\beta^2-4a\beta)A+(\beta-a)^2p^2B), \\
(8) : & -p^2g^2a^2(1-\gamma^2)^2N_f\delta^{ab}\frac{3}{4}B,
\end{aligned}$$

FIG. 8: Contributions to  $\Pi_{\pi p}$  at one-loop.

$$\begin{aligned}
(9) &: \frac{-p^2}{\beta} g^2 N_f \delta^{ab} (a - \beta)^2 \gamma^2 \frac{3}{4} B, \\
(10) &: \frac{-p^2 \gamma^2}{a} g^2 N_f \delta^{ab} (\beta - a)^2 \frac{3}{4} B, \\
(11) &: F_\pi^2 g^4 (\beta - a)^2 \gamma^2 N_f \delta^{ab} (D - 1) B.
\end{aligned} \tag{C.96}$$

The sum of divergent parts is given by

$$\begin{aligned}
\Pi_{\pi\pi}|_{\text{div}} = & -N_f \frac{p^2}{F_\pi^2} \left[ A \left( -\frac{4 - 3a(1 - \gamma^2)^2}{12} + \frac{\beta \gamma^2}{a} + \frac{\gamma^2}{\beta} \frac{1}{4} a + \frac{a(1 - \gamma^2)^2}{4} + \frac{\gamma^2}{4a\beta} (-4\beta a - 2\beta^2 + a^2) \right) \right. \\
& \left. - B F_\pi^2 g^2 \frac{3}{4} \left( a^2 (1 - \gamma^2)^2 + \gamma^2 (a - \beta)^2 \left( \frac{1}{\beta} + \frac{1}{a} \right) \right) + \frac{1}{4} p^2 B \left( a(1 - \gamma^2)^2 + \frac{\gamma^2}{a\beta} (\beta - a)^2 \right) \right]. \tag{C.97}
\end{aligned}$$

The divergences are canceled out by the following counterterms:

$$\Pi_{\pi\pi}|_{\text{div}} = p^2 (\delta_{Z_\pi} + p^2 \delta_{4\pi\pi}), \tag{C.98}$$

where  $\delta_{4\pi\pi}$  is the counter term from the  $\mathcal{O}(p^4)$  Lagrangian.

## 8. $\pi - p$

The contributions from each diagram shown in Fig. 8 are

$$(1) : \text{Diagram 1} = -\frac{\gamma}{2\sqrt{\beta}} \frac{2\beta - 3a}{6} (1 - \gamma^2) \frac{p^2}{F_\pi^2} N_f \delta^{ab} A(0), \tag{C.99}$$

$$(2) : \text{Diagram 2} = \frac{\gamma}{2\sqrt{\beta}} \frac{\beta}{a} \frac{p^2}{F_\pi^2} N_f \delta^{ab} A(0), \tag{C.100}$$

$$(3) : \text{Diagram 3} = \frac{\gamma}{2\sqrt{\beta}} \frac{a - 2\beta}{6\beta} \frac{p^2}{F_\pi^2} N_f \delta^{ab} A(0), \tag{C.101}$$

$$(4) : \text{Diagram 4} = \frac{\gamma}{2\sqrt{\beta}} 2g^2 (a - \beta) 3N_f \delta^{ab} A(M_\rho^2), \tag{C.102}$$

$$(5) : \text{Diagram 5} = \frac{\gamma}{2\sqrt{\beta}} 2g^2 (\beta - a) 3N_f \delta^{ab} A(M_{A_1}^2), \tag{C.103}$$

$$(6) : \text{Diagram 6} = \frac{\gamma}{2\sqrt{\beta}} \frac{-1}{2} (1 - \gamma^2) \frac{p^2}{F_\pi^2} N_f \delta^{ab} ((a + 2\beta)A(0) + (a + \beta)p^2 B(p, 0, 0)), \tag{C.104}$$

$$(7) : \text{Diagram 7} = \frac{\gamma}{2\sqrt{\beta}} \frac{1}{2\beta} \frac{p^2}{F_\pi^2} N_f \delta^{ab} ((a - 2\beta)A(0) + (a - \beta)p^2 B(p, 0, 0)), \tag{C.105}$$



$$(8) : \text{---} \circlearrowleft[\rho]{\pi} \text{---} = \frac{\gamma}{2\sqrt{\beta}} 2g^2 a(1-\gamma^2)(a-\beta) N_f \delta^{ab} \left( p^2 B(p, 0, M_\rho^2) - \frac{p^\mu p^\nu}{M_\rho^2} \left( \tilde{B}_{\mu\nu}(p, 0, M_\rho^2) - \tilde{B}_{\mu\nu}(p, 0, 0) \right) \right), \quad (\text{C.106})$$

$$(9) : \text{---} \circlearrowleft[\rho]{p} \text{---} = \frac{\gamma}{2\sqrt{\beta}} 2g^2 \frac{(2\beta-a)}{\beta} (a-\beta) N_f \delta^{ab} \left( p^2 B(p, 0, M_\rho^2) - \frac{p^\mu p^\nu}{M_\rho^2} \left( \tilde{B}_{\mu\nu}(p, 0, M_\rho^2) - \tilde{B}_{\mu\nu}(p, 0, 0) \right) \right), \quad (\text{C.107})$$

$$(10) : \text{---} \circlearrowleft[A_1]{\sigma} \text{---} = \frac{\gamma}{2\sqrt{\beta}} 2g^2 (\beta-a) N_f \delta^{ab} \left( p^2 B(p, 0, M_\rho^2) - \frac{p^\mu p^\nu}{M_\rho^2} \left( \tilde{B}_{\mu\nu}(p, 0, M_\rho^2) - \tilde{B}_{\mu\nu}(p, 0, 0) \right) \right), \quad (\text{C.108})$$

$$(11) : \text{---} \circlearrowleft[\rho]{A_1} \text{---} = \frac{\gamma}{2\sqrt{\beta}} 2g^4 F_\pi^2 (a-\beta)^2 N_f \delta^{ab} \left( 3B(p, M_\rho^2, M_{A_1}^2) - \frac{p^2}{M_{A_1}^2} (B(p, M_{A_1}^2, M_\rho^2) - B(p, 0, M_\rho^2)) \right) + \frac{p^\mu p^\nu}{M_{A_1}^2 M_\rho^2} (\tilde{B}_{\mu\nu}(p, M_{A_1}^2, M_\rho^2) - \tilde{B}_{\mu\nu}(p, 0, M_\rho^2)). \quad (\text{C.109})$$

The divergent parts are given by

$$\begin{aligned} (1) : & \frac{\gamma}{2\sqrt{\beta}} \frac{2\beta-3a}{6} (1-\gamma^2) \frac{p^2}{F_\pi^2} N_f \delta^{ab} A, \\ (2) : & \frac{\gamma}{2\sqrt{\beta}} \frac{\beta}{a} \frac{p^2}{F_\pi^2} N_f \delta^{ab} A, \\ (3) : & \frac{\gamma}{2\sqrt{\beta}} \frac{a-2\beta}{6\beta} \frac{p^2}{F_\pi^2} N_f \delta^{ab} A, \\ (4) : & \frac{\gamma}{2\sqrt{\beta}} 2g^2 (a-\beta) 3N_f \delta^{ab} (A - M_\rho^2 B), \\ (5) : & \frac{\gamma}{2\sqrt{\beta}} 2g^2 (\beta-a) 3N_f \delta^{ab} (A - M_{A_1}^2 B), \\ (6) : & \frac{\gamma}{2\sqrt{\beta}} \frac{-1}{2} (1-\gamma^2) \frac{p^2}{F_\pi^2} N_f \delta^{ab} ((a+2\beta)A + (a+\beta)p^2 B), \\ (7) : & \frac{\gamma}{2\sqrt{\beta}} \frac{1}{2\beta} \frac{p^2}{F_\pi^2} N_f \delta^{ab} ((a-2\beta)A + (a-\beta)p^2 B), \\ (8) : & \frac{\gamma}{2\sqrt{\beta}} g^2 a(1-\gamma^2)(a-\beta) N_f \delta^{ab} p^2 \frac{3}{2} B, \\ (9) : & g^2 \frac{(2\beta-a)}{\beta} (a-\beta) N_f \delta^{ab} p^2 \frac{3}{2} B, \\ (10) : & \frac{g^2 \gamma}{2\sqrt{\beta}} (\beta-a) N_f \delta^{ab} p^2 \frac{3}{2} B, \\ (11) : & \frac{\gamma}{2\sqrt{\beta}} 2g^4 F_\pi^2 (a-\beta)^2 3N_f \delta^{ab} B. \end{aligned} \quad (\text{C.110})$$

The sum of divergent parts is given by

$$\begin{aligned} \Pi_{\pi p}|_{\text{div}} = & \frac{\gamma}{2\sqrt{\beta}} \frac{p^2}{F_\pi^2} N_f \delta^{ab} \left[ A \left( \left( \frac{1}{3}\beta - \frac{1}{2}a \right) (1-\gamma^2) + \frac{\beta}{a} + \frac{-1}{\beta} \left( \frac{1}{3}\beta - \frac{1}{2}a \right) - (1-\gamma^2) \frac{1}{2} (a+2\beta) + \frac{1}{2\beta} (a-2\beta) \right) \right. \\ & + 2F_\pi^2 \frac{3}{4} g^2 B \left( -a(1-\gamma^2)(\beta-a) + \frac{(2\beta-a)}{\beta} (a-\beta) + (\beta-a) \right) \\ & \left. + \frac{p^2}{2} B(-(1-\gamma^2)(a+\beta) + \frac{1}{\beta} (a-\beta)) \right]. \end{aligned} \quad (\text{C.111})$$

The divergences are canceled out by the following counterterms:

$$\Pi_{\pi p}|_{\text{div}} = p^2 (-\delta_{\pi p} + p^2 \delta_{4\pi p}), \quad (\text{C.112})$$

where  $\delta_{4\pi p}$  is the counterterm from  $\mathcal{O}(p^4)$ .

## APPENDIX D: RENORMALIZATION GROUP EQUATIONS

The renormalization group equation for the parameter  $\lambda_i = F_\pi^2, a, \beta, \dots$ , at one loop is given by

$$\mu \frac{d\lambda_i}{d\mu} = \Lambda \frac{d\delta\lambda_i}{d\Lambda} \Big|_{\Lambda=\mu}, \quad (\text{D.1})$$

where  $\delta\lambda_i$  is counter term for  $\lambda_i$ . From Eqs.(C.12), (C.23), (C.33), (C.46), (C.68), (C.84), (C.98) and (C.112), we obtain the renormalization group equations as follows:

$$\begin{aligned} \mu \frac{dF_\pi^2}{d\mu} &= \frac{2N_f}{(4\pi)^2} \left[ \mu^2 \left( 1 - \frac{a}{2} + \gamma^2 + a\gamma^2 - \frac{a\gamma^2}{2\beta} - \frac{\beta\gamma^2}{2a} - \frac{a\gamma^4}{2} \right) \right. \\ &\quad \left. + \frac{3}{4} F_\pi^2 g^2 \left( a^2 - a\gamma^2 - 2a^2\gamma^2 + \frac{a^2\gamma^2}{\beta} - \beta\gamma^2 + \frac{\beta^2\gamma^2}{a} + a^2\gamma^4 \right) \right], \\ \mu \frac{dF_\sigma^2}{d\mu} &= \frac{2N_f}{(4\pi)^2} \left[ \mu^2 \left( \frac{1}{4} + \frac{a^2}{4} + \frac{a^2}{4\beta^2} - \frac{a^2\gamma^2}{2} + \frac{a^2\gamma^2}{2\beta} - \frac{\beta\gamma^2}{2} + \frac{a^2\gamma^4}{4} \right) \right. \\ &\quad \left. + \frac{3}{4} F_\pi^2 g^2 \left( a + \frac{a^2}{\beta} + a^2\gamma^2 + \beta^2\gamma^2 - 2a\beta\gamma^2 \right) \right], \\ \mu \frac{dF_{A_1}^2}{d\mu} &= \frac{2N_f}{(4\pi)^2} \gamma^2 \left[ \mu^2 \left( -1 - a + \frac{a}{2\beta} + \frac{\beta}{a} + \frac{a\gamma^2}{2} + \frac{\beta^2\gamma^2}{2a} \right) \right. \\ &\quad \left. + \frac{3}{4} F_\pi^2 g^2 \left( a + 2a^2 - \frac{a^2}{\beta} - 2a\beta - a^2\gamma^2 + \beta^2\gamma^2 + 2\beta \right) \right], \\ \mu \frac{dF_p^2}{d\mu} &= \frac{2N_f}{(4\pi)^2} \left[ \mu^2 \left( 1 - \frac{a}{2\beta} - \frac{a\gamma^2}{2} + \frac{\beta^2\gamma^2}{2a} \right) \right. \\ &\quad \left. + \frac{3}{4} F_\pi^2 g^2 \left( -3a + \frac{a^2}{\beta} + 4\beta + a^2\gamma^2 - 2a\beta\gamma^2 + \beta^2\gamma^2 \right) \right], \\ \mu \frac{dg^2}{d\mu} &= -2g^4 \frac{N_f}{(4\pi)^2} \left[ \frac{22}{3} - \frac{1}{48} \left( 5 + a^2 + \frac{a^2}{b^2} - \frac{2a}{\beta} - 2a\gamma^2 - 2a^2\gamma^2 + \frac{2a^2\gamma^2}{\beta} - 2\beta\gamma^2 + \frac{2\beta^2\gamma^2}{a} + a^2\gamma^4 \right) \right], \\ \mu \frac{dz_1}{d\mu} &= \frac{N_f}{(4\pi)^2} \frac{1}{24} \left( 5 - 4a + a^2 + \frac{a^2}{\beta^2} - 2a^2\gamma^2 + \frac{2a^2\gamma^2}{\beta} + 2\beta\gamma^2 + a^2\gamma^4 \right), \\ \mu \frac{dz_2}{d\mu} &= \frac{N_f}{(4\pi)^2} \frac{1}{12} \left( a - 2\beta\gamma^2 + \frac{\beta\gamma^2}{a} + \frac{\beta^2\gamma^4}{a} \right), \\ \mu \frac{dz_3}{d\mu} &= \frac{N_f}{(4\pi)^2} \frac{1}{12} \left( 1 + 2a - a^2 - \frac{a^2}{\beta^2} + \frac{2a}{\beta} + 2a\gamma^2 + 2a^2\gamma^2 - \frac{2a^2\gamma^2}{\beta} - 2\beta\gamma^2 - a^2\gamma^4 \right), \\ \mu \frac{dz_4}{d\mu} &= \frac{N_f}{(4\pi)^2} \frac{1}{6} \gamma \left( 1 - a + \beta + \beta\gamma^2 - \frac{\beta^2\gamma^2}{a} \right), \\ \mu \frac{d\kappa}{d\mu} &= \frac{N_f}{(4\pi)^2} \frac{g^2}{48} \left( -5 - a^2 - \frac{a^2}{\beta^2} + \frac{6a}{\beta} + 6a\gamma^2 + 2a^2\gamma^2 - \frac{2a^2\gamma^2}{\beta} - 6\beta\gamma^2 + \frac{2\beta^2\gamma^2}{a} - a^2\gamma^4 \right) \end{aligned} \quad (\text{D.2})$$

We define the parameter to calculate the RGEs for the dimensionless parameter for convenience:

$$\begin{aligned} x(\mu) &= \frac{N_f}{(4\pi)^2} \frac{\mu^2}{F_\pi^2}, \\ G(\mu) &= \frac{N_f}{(4\pi)^2} g^2. \end{aligned} \quad (\text{D.3})$$

The beta functions for the dimensionless parameters  $x, a, \beta, \gamma^2, G$  are given by

$$\begin{aligned}
\beta_x &= x(2 - \frac{1}{F_\pi^2} \mu \frac{dF_\pi^2}{d\mu}), \\
\beta_a &= \frac{1}{F_\pi^2} (\mu \frac{dF_\sigma^2}{d\mu} - \mu \frac{dF_\pi^2}{d\mu} a), \\
\beta_\beta &= \frac{1}{F_\pi^2} (\mu \frac{dF_p^2}{d\mu} - \mu \frac{dF_\pi^2}{d\mu} \beta), \\
\beta_{\gamma^2} &= \frac{1}{\beta F_\pi^2} (\mu \frac{dF_{A_1}^2}{d\mu} - \mu \frac{dF_p^2}{d\mu} \gamma^2), \\
\beta_G &= \frac{N_f}{(4\pi)^2} \mu \frac{dg^2}{d\mu}.
\end{aligned} \tag{D.4}$$

We obtain the RGEs in Eq.(4.3) by combining Eqs.(D.2) and (D.4).

- 
- [1] T. Hatsuda and T. Kunihiro, Phys. Rept. **247**, 221 (1994).
  - [2] R. Rapp and J. Wambach, Adv. Nucl. Phys. **25**, 1 (2000).
  - [3] G. E. Brown and M. Rho, Phys. Rept. **363**, 85 (2002).
  - [4] G. Agakichiev *et al.* [CERES Collaboration], Phys. Rev. Lett. **75**, 1272 (1995).
  - [5] F. Bonutti *et al.* [CHAOS Collaboration], Phys. Rev. Lett. **77**, 603 (1996); F. Bonutti *et al.* [CHAOS collaboration], Nucl. Phys. A **677**, 213 (2000).
  - [6] K. Ozawa *et al.* [E325 Collaboration], Phys. Rev. Lett. **86**, 5019 (2001); M. Naruki *et al.*, arXiv:nucl-ex/0504016.
  - [7] E. Scomparin, Plenary talk at Quark Matter 2005.
  - [8] M. Harada and K. Yamawaki, Phys. Rev. Lett. **86**, 757 (2001)
  - [9] G. E. Brown and M. Rho, Phys. Rev. Lett. **66**, 2720 (1991).
  - [10] M. Bando, T. Kugo, S. Uehara, K. Yamawaki and T. Yanagida, Phys. Rev. Lett. **54**, 1215 (1985).
  - [11] M. Bando, T. Kugo and K. Yamawaki, Nucl. Phys. B **259**, 493 (1985).
  - [12] M. Bando, T. Kugo and K. Yamawaki, Prog. Theor. Phys. **73**, 1541 (1985).
  - [13] T. Fujiwara, T. Kugo, H. Terao, S. Uehara and K. Yamawaki, Prog. Theor. Phys. **73**, 926 (1985).
  - [14] M. Bando, T. Fujikawa, and K. Yamawaki, Prog. Theor. Phys. **79**, 1140 (1988)
  - [15] C. N. Yang and R. L. Mills, Phys. Rev. **96**, 191 (1954).
  - [16] J. J. Sakurai, Currents and Mesons, Chicago University Press, Chicago, (1969).
  - [17] J. S. Schwinger, Phys. Lett. B **24**, 473 (1967).
  - [18] J. Wess and B. Zumino, Phys. Rev. **163**, 1727 (1967).
  - [19] S. Weinberg, Phys. Rev. **166**, 1568 (1968).
  - [20] J. Gasser and H. Leutwyler, Annals Phys. **158**, 142 (1984).
  - [21] G. Ecker, J. Gasser, A. Pich and E. de Rafael, Nucl. Phys. B **321**, 311 (1989).
  - [22] M. Tanabashi, Phys. Lett. B **316**, 534 (1993).
  - [23] M. Harada and K. Yamawaki, Phys. Rev. Lett. **83**, 3374 (1999).
  - [24] M. Harada and K. Yamawaki, Phys. Rev. D **64**, 014023 (2001)
  - [25] M. Harada and C. Sasaki, Phys. Lett. B **537**, 280 (2002).
  - [26] M. Harada, Y. Kim and M. Rho, Phys. Rev. D **66**, 016003 (2002).
  - [27] F. J. Gilman and H. Harai, Phys. Rev. **165**, 1803 (1968)
  - [28] S. Weinberg, Phys. Rev. **177**, 2604 (1969)
  - [29] S. Weinberg, Phys. Rev. Lett. **65**, 1177 (1990).
  - [30] K. Yamawaki, arXiv:hep-th/9802037.
  - [31] M. Bando, T. Kugo and K. Yamawaki, Phys. Rept. **164**, 217 (1988).
  - [32] STAR Collaboration, Phys. Rev. Lett. **92**, 092301 (2004)
  - [33] G. E. Brown, C. H. Lee and M. Rho, arXiv:nucl-th/0507073.
  - [34] M. Harada and K. Yamawaki, Phys. Lett. B **297**, 151 (1992).
  - [35] M. Harada and K. Yamawaki, Phys. Rept. **381**, 1 (2003).
  - [36] M. A. Shifman, A. I. Vainshtein and V. I. Zakharov, Nucl. Phys. B **147**, 385 (1979).
  - [37] M. A. Shifman, A. I. Vainshtein and V. I. Zakharov, Nucl. Phys. B **147**, 448 (1979).
  - [38] S. Weinberg, Phys. Rev. **177**, 2604 (1969).
  - [39] M. Harada and C. Sasaki, arXiv:hep-ph/0511312.
  - [40] H. Georgi, Phys. Rev. Lett. **63**, 1917 (1989).
  - [41] T. Hatsuda and T. Kunihiro, Phys. Rev. Lett. **55**, 158 (1985).
  - [42] S. Chiku and T. Hatsuda, Phys. Rev. D **58**, 076001 (1998).

- [43] Y. Hidaka, O. Morimatsu, T. Nishikawa and M. Ohtani, Phys. Rev. D **68**, 111901 (2003).